NANO-CELLULOSE REINFORCED SHEET MOLDING COMPOUNDS FOR AUTOMOTIVE COMPOSITE MANUFACTURING

A Thesis
Presented to
The Academic Faculty

by

Mark Miller

In Partial Fulfillment
of the Requirements for the Degree
Mechanical Engineering in the
School of Woodruff School of Mechanical Engineering

Georgia Institute of Technology
August 2016

NANO-CELLULOSE REINFORCED SHEET MOLDING COMPOUNDS FOR AUTOMOTIVE COMPOSITE MANUFACTURING

Approved by:

Dr. Kyriaki Kalaitzidou, Advisor
School of Materials Science and Engineering
Georgia Institute of Technology

Dr. Robert Moon
School of Materials Science and Engineering
Georgia Institute of Technology

Dr. Jonathan Colton
School of Mechanical Engineering
Georgia Institute of Technology

Date Approved: 05/19/2016

[To the Georgia Institute of Technology]

ACKNOWLEDGMENTS

I would like to thank my mother, father, and my two younger brothers, whom kept me grounded throughout my entire career at Georgia Tech. I would like to also thank my close friends whom I consider to be family, who believed in me even when times were difficult. I would like to thank my graduate advisor, Dr. Kyriaki Kalaitzidou, for constructing a program that would provide an enriching experience, and Dr. Robert Moon and Dr. Jonathan Colton for giving me guidance throughout my Master's program. I would also like to thank Dr. Amir Asadi for working closely alongside me and teaching me how to operate the various characterization machines. Finally, I would like to thank P^3 Nano and the U.S. Forestry Endowment for the funding of this project.

TABLE OF CONTENTS

LIST OF TABLES

LIST OF FIGURES

LIST OF SYMBOLS AND ABBREVIATIONS

PMC	Polymer Matrix Composites
SMC	Sheet Molding Compound
CN	Cellulose Nanomaterial
WF/PF	Wood Fiber
MCC	Microcrystalline Cellulose
AC	Algae Cellulose Particles
MFC	Microfibrillated Cellulose
NFC	Nanofibrillated Cellulose
CNC	Cellulose Nanocrystal
t-CNC	Tunicate Cellulose Nanocrystal
GF	Glass Fiber
SWNT	Single Walled Nanotube
MWNT	Multi Walled Nanotube
SFFT	Single Fiber Fragmentation Test
IFSS	Interfacial Shear Strength
SEM	Scanning Electron Microscope
TGA	Thermogravimetric Analysis
DMA	Dynamic Mechanical Analysis

SUMMARY

The focus of this research is to investigate the potential of cellulose nanocrystals (CNC) as reinforcement in typical glass fiber/epoxy sheet molding compounds (SMC). The hypothesis is that addition of CNC can improve the properties of the SMC composites, allowing glass fibers to be removed thus reducing the density/weight of the composite without compromising its mechanical properties. Reducing the weight of materials, including composites, can lead to better performance of the materials and/or higher fuel efficiency in case of materials used for transportation applications. In this research CNC is added into the glass fiber/epoxy systems either as a coating of the glass fibers or directly to the resin. In case of the CNC-coated glass fibers, the coating is characterized using optical and scanning electron microscopy, single fiber fragmentation tests and thermogravimetric analysis. The CNC-glass fiber/epoxy composites are made and their mechanical properties and density are determined as a function of the CNC content. Furthermore, a fiber coating bath that is connected to the SMC manufacturing line to enable in-stream coating and production of these composites using the SMC technology is designed and built based on feedback from the coating study. In case of adding the CNC in the resin, the composites were made using the SMC manufacturing line and their mechanical properties, density and structure were characterized as a function of the CNC content. In conclusion, addition of CNC either as a glass fiber coating or as an additive to the resin results in composites with improved tensile and flexural strength and modulus, does not alter the impact strength and the density and lays the ground for light-weighting of fiber reinforced polymer composites.

CHAPTER 1

INTRODUCTION

Fiber-reinforced polymer matrix composites have had widespread use in automotive, aviation, and marine vehicles due to their high strength-to-weight ratios, rigidities, and formable capabilities. The use of composites with approximately 30-50% fiber loading has enabled these industries to produce products that are not only light-weight, but are also strong and durable for their individual specific uses for the past 40 years. Development of these materials is primarily driven by the premise that a 10% reduction in vehicle weight results in a 6-8% increase in fuel efficiency [1]. This has become especially important as the cost of energy has increased in recent years. Lightweight does not translate only to improved fuel efficiency but to better performance i.e., increased speed of vehicles, which is equally important in the very competitive recreational transportation industry.

Sheet molding compounds (SMC) manufacturing technology, which impregnates the fibrous materials between two layers of a thermosetting resin, has been the primary manufacturing method for producing composites since the 1970s due to its high-volume application, part reproduction capability, surface finish quality, cost effectiveness, autonomy, and low material waste. Ultimately, these various industries look to light-weight the composites produced by the SMC process by replacing the heavier components (i.e., fibrous material) with lighter components (i.e., nanoparticles) without compromising the mechanical properties of the material. Many studies have explored the usage of nanomaterials within polymer matrix composites to achieve this goal.

1.1 Introduction to Nanomaterials

In recent years, nano-materials have been the main point of interest in achieving the necessary increase in material performance to significantly reduce the overall weight of the manufactured composites. There have been two main mechanisms in which nanoparticles are incorporated into polymer matrix composites: as a reinforcement phase within the matrix polymer, and as an interface between the fibers and the matrix [2-5]. The high surface-area-to-volume ratio for nanoparticles allow for enhanced interactions between the other constituents in the composite, resulting in enhanced load distribution management within the composite as compared to a homogeneous matrix [6]. However, several challenges are present for fully utilizing nanoparticles within industrial composites, such as outfitting existing SMC lines to incorporate nanoparticles and inhomogeneous dispersion of the nanomaterials within the composite due to agglomerate formation. These issues must be addressed before nanomaterials can be seen as a viable option for industrial composite enhancement.

Polymer nano-composites are polymer matrix composites in which one of the reinforcements has dimensions in the nanometer range [7]. Three popular nano-reinforcements that are currently used to manufacture polymer nano-composites are nanoclays, carbon nanofibers, and carbon nanotubes. Each of the nano-reinforcements has different effects on the nanocomposite, and different dispersion methods as well, which will be explained to give a background on the current usage and benefits of nano-reinforcements.

Nano-clay composites are made from layered silicate clay mineral, such as smectite clay [8]. Smectite clay particles have natural dimensions of 6-10 μm and contain

more than 3000 layers. However, these particles are able to be either exfoliated or delaminated into individual layers that are about 1 nm thick. When mixed with a polymer, there are three possible types of dispersion resulting in the following structures: intercalated, exfoliated, and phase-separated structure. Intercalated dispersion occurs when one or more of the polymer molecules are intercalated between the silicate layers with spacing of 2-3 nm [9-10]. Exfoliated dispersion occurs when the silicate layers are completely delaminated and uniformly dispersed throughout the polymer matrix with spacing of 8-10 nm. This type of dispersion is most desirable for reinforcing the polymer matrix. Phase-separated dispersion occurs when the polymer matrix is unable to delaminate or intercalate between the silicate layers, resulting in multiple phases within the composite. This outcome is least desirable for reinforcement.

There are three main methods of dispersing nanoclays within the polymer, the solution method, the *in-situ* polymerization and the melt-processing method. The solution method involves delaminating the silicate layers in a solvent in which the polymer can be dissolved. Once the polymer is added to the solution and the solvent is evaporated, the result is the polymer intercalated between the silicate layers. The *in situ* polymerization method involves swelling the silicate layers within the monomer, and then later polymerized by heat or radiation. This method is mainly used for thermosetting resins, such as epoxy. Finally, the melt processing method describes a process in which the nanoclays are mixed into the polymer at a liquid/melt state. Research results from Toyota suggests that the addition of 5% of exfoliated nanoclays increases the tensile strength by 38 MPa, and the tensile modulus by 1.0 GPa [10]. However, non-exfoliated nanoclays had not yielded any mechanical improvements to the polymer matrix.

Carbon nanofibers are made either by vapor-grown techniques or by electrospinning [11-13]. They are typically 20-200 nm in diameter and 30-100 μm in length. Carbon nanofibers are available in several different morphologies, the most common being platelet in which the graphitic layers are perpendicular to the fiber axis, hollow tubular, in which the graphitic layers are parallel to the fiber, and fishbone, in which the graphitic layers are 10-40 degrees at an angle to the fiber axis.

Carbon nanofibers have been incorporated into several different thermoplastics and thermosets, with their effect on mechanical properties being inconclusive [14-15]. The general trend is that carbon nanofibers yield increased strength and modulus in thermoplastics and significantly reduced property enhancement in thermosets. Finegan et al. conducted a study on the tensile properties of carbon nanofiber-reinforced polypropylene, in which various production conditions and surface treatments of the nanofibers were observed [14]. In all of the cases, the tensile strength and modulus of the polypropylene were increased, however the magnitude of the increase was effected by the processing condition and surface treatment of the nanofibers used. Patton et al. conducted a study on nanofiber reinforced-epoxy, in which the epoxy was diluted with acetone and then infused into a carbon nanofiber mat. The resulting composite had a flexural modulus that increased by 100%, and a flexural strength that increased by 36% when compared to homogeneous epoxy [15].

Carbon nanotubes were discovered in 1991 and have attracted many researchers due to their potential as reinforcement for structural composites, energy storage devices, electronic systems, biosensors, and drug delivery systems [16-17]. Their unique structure yields exceptional mechanical and thermal properties. Their elastic modulus is higher

than 1TPa, which is 3-4 times greater than that of carbon nanofibers [18]. There are two different morphologies for carbon nanotubes: single walled nanotubes (SWNT) and multi-walled nanotubes (MWNT) [18]. SWNT is a seamless, hollow cylinder, while MWNT consist of a number of concentric SWNT. Both morphologies are closed at the ends by dome-shaped caps. There are three methods for producing carbon nanotubes, electric arc discharge, laser ablation, and chemical vapor deposition [17]. Carbon nanotubes must be functionalized to improve their dispersion within a polymer matrix, create better bonding with the polymer matrix, and to increase their solubility in solvents [7]. They may be functionalized by oxidation, fluoridation, amidation, or other chemical reactions to covalently bond the functional groups to either the walls or the ends.

Much like nanoclays, carbon nanotubes can be dispersed within a polymer matrix by means of *in situ* polymerization, solution processing, and melt compounding [19-20]. For *in situ* polymerization, the nanotubes are dispersed into the monomer, and then the composite is created by initiating the polymerizing reaction. In solution processing, the nanotubes are first dispersed within a solvent in which the polymer is soluble, and then the polymer is added to the solution, and mixed using either magnetic stirring, high-shear mixing, or sonication. The solution is then cast into a mold, and the solvent is allowed to evaporate. Melt processing for carbon nanotubes is implemented by blending the nanotubes with the melted polymer using a high-shear mixer or an extruder, followed by pelletizing and compression molding or by injection molding. Melt compounding is the preferred process for high-volume applications.

Based on the superior mechanical properties of the nanotubes, it is expected that the resulting composites will exhibit a very high modulus and strength. Many studies

have verified that properly dispersed nanotubes have a significant effect on the mechanical properties when compared to the neat polymer. The following two examples exemplify this. In the first example, 5 wt% MWNT was dispersed into polystyrene using the solution processing method with toluene [21]. The resulting composite had a modulus increase of 120% and a tensile strength increase of 56%. In the second example, 1 wt% MWNT was dispersed via melt processing into polyamide-6 [22]. The resulting composite had a modulus increase of 115% and a strength increase of 124%. From each of these examples, it is clear to see that the addition of nanomaterials to neat composites have a positive significant effect on the mechanical properties of the composite.

Alternative nanoparticles that also have potential for increasing polymer-matrix composites are cellulose nanomaterials (CNs). CNs are cellulose-based nanoparticles obtained from plants, algae, bacteria, and marine animals [23]. CNs must be isolated from their individual sources, usually by means of mechanical treatment or acid hydrolysis. Nine particle types are considered to be the main cellulose-based nanoparticles based on the extraction sources and the isolation process. These types are wood fiber (WF/PF), microcrystalline cellulose (MCC), microfibrillated cellulose (MFC), nanofibrillated cellulose (NFC), cellulose nanocrystals (CNC), tunicate cellulose nanocrystals (t-CNC), algae cellulose particles (AC), and bacterial cellulose particles (BC) [23]. CNs have gained considerable interest in recent years due to their low density, high surface area and aspect ratio, tensile strength, elastic modulus, functionalization capabilities, and low toxicity. In addition, because CNs are the most naturally occurring polymers in the world, their extraction and utility is sustainable, renewable, recyclable, widely available, biodegradable, and low cost [24]. CNs have the potential of developing

light-weight, environmentally-friendly, structural composites. The specific CN used in this study to verify the potential of using such nanomaterials in composites for high volume automotive applications is cellulose nanocrystals (CNC).

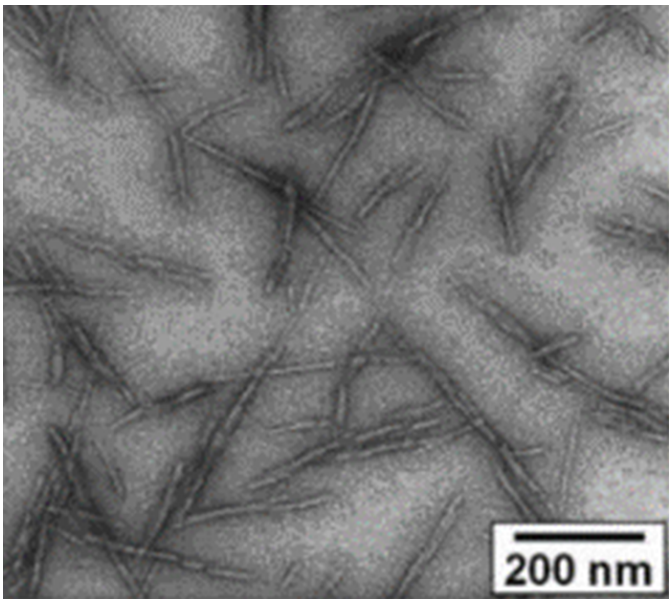

Figure 1.1: TEM Image of CNC [24]

CNC are rod-or-whisker shaped particles generated from the acid hydrolysis of WF, MCC, MFC, or NFC. CNC have a high aspect ratio (3-5 nm in width, and 5-500 nm in length), and are highly crystalline. A TEM image of CNC nanoparticles is shown in Figure 1. Amorphous regions may occur within the CNC if there is incomplete hydrolysis. In addition, CNC may also depolymerize if the hydrolysis is too harsh. CNC tend to agglomerate as well, based on the sample preparation method. Rusli et al. [25] had utilized Raman spectroscopy to determine the axial modulus to be 57 GPa or 105 GPa, depending on whether they are arranged in a 2D or 3D network, respectively. The high modulus of the CNC in the axial direction suggests that they will have a significant effect on the mechanical properties should they be properly dispersed or incorporated into the composite.

CNC are currently used commercially for several practically useful products. Commercial forms of microcrystalline cellulose as a colloidal system are available as an aqueous solution at high solid concentration, providing a 10 wt % slurry of cellulose nanofibers [26]. Solidified liquid CNC have been applied for optical applications such as security paper [26]. Organic light emitting diodes (OLEDs) are manufactured from wood cellulose nanocomposites [26]. Cellulose whiskers are also employed for low thickness polymer electrolytes for lithium batteries [26].

While CNC have clear optical and electrical benefits, several studies have been conducted to observe the mechanical benefits of incorporating CNC into polymers and composites. Al-Turaif et al. [27] conducted a study with NFC-reinforced epoxy, in which the tensile strength, elongation, toughness, and Young's modulus were investigated. For this study, the NFC was mechanically mixed into the epoxy resin directly. At 0.1 wt%, the maximum stress increased by 120%, the strain to failure increased by 73%, the toughness increased by 300%, and the Young's modulus increased by 64% in comparison to the neat epoxy resin. The improvement of the mechanical properties was attributed to the dispersion in the epoxy matrix and the adhesion of the NFC to the epoxy. At low fiber concentrations, increased mechanical properties are observed, however at higher concentrations, agglomeration occurs, in which uniform dispersion is impossible, thus decreasing the mechanical properties of the composite. Low et al. [28] conducted a study in which epoxy laminates reinforced by cellulose fiber mats (CFM) were investigated. As observed, the strain-at-break, fracture toughness, and impact toughness increased by several orders of magnitude, and moderate gains were observed in the flexural strength and modulus. This increase in mechanical properties is attributed to increased energy

dissipation at the epoxy-fiber interface. Tang et al. [29] prepared samples of CNC-reinforced epoxy by using the solvent exchange method, in which 20% v/v CNC at 180ºC yielded a 2000% increase in tensile modulus as compared to neat epoxy. From these results, improvement of mechanical properties from CNC-reinforcement is promising.

Additional work is required to identify a viable solution for incorporating CNC in composites made using scalable processing methods commonly employed by industry for high volume applications including automotive and aerospace products. One such method is sheet molding compound (SMC) processing and manufacturing of composites using SMC.

1.2 Goal and Objectives

The goal of this research is to introduce CNC in composites made by compression molding of SMC and investigate the effect of the CNC on the mechanical properties, including tensile and flexural modulus and strength and impact strength, and density of the resulting composites. The properties will be characterized as a function of the CNC content and the method the CNC were added into the composites. Two such methods are investigated: i) addition of CNC as a coating of the glass fibers and ii) addition of CNC in the resin. The hypothesis that CNC coating of glass fibers enhances the interfacial interactions with the resin and the propertied of CNC-coated glass fiber/epoxy composites is confirmed by making composites using lab-scale techniques and characterize their properties. A fiber-coating bath is designed and built using feedback from the lab-scale coating study, and it is integrated to the SMC manufacturing line.

Chapter 2 describes the process for material selection and provides details on the SMC line used in this study including all the calibration process. The lab-scale study

where GF are coated with CNC and composites are made and characterized, along with the bath design for scalable fiber coating are presented in Chapter 3. Chapter 4 includes the study on addition of CNC into the resin and making composites using the SMC line. Finally Chapter 5 provides a summary of the results and some recommendations as to what needs to be done next in order to demonstrate the light-weighting effect the addition of CNC can have on SMC composites.

CHAPTER 2

ADDITION OF CNC INTO THE SMC AND CALIBRATION OF THE SMC LINE

2.1 Addition of CNC into SMC

All of the previous examples of nanoparticles being incorporated into polymer matrix composites had assumed proper dispersion to observe a significant increase in mechanical properties. However, this is exceedingly challenging for CN for most epoxy systems due to their hydrophilicity. To address this issue, waterborne epoxies [31-32], solvent exchange methods [33-35], and surface functionalization via chemical modification [36] have been utilized to fully incorporate the CN within the epoxy systems. Waterborne epoxies take full advantage of CN hydrophilicity, and allow CN to be applied directly to the epoxy, and mechanical mixing will in fact fully disperse them within the epoxy. The solvent exchange method involves a process in which a non-polar solvent (i.e., acetone) would be added to an aqueous CN solution, and over time, a layer of the CN-acetone mixture would be present within the mixture. Finally, once a mechanically coherent mixture of the CN-acetone mixture is present, it can be mechanically removed and applied to an epoxy for full dispersion [29]. Finally, surface functionalization via chemical modification involves a process that "changes" the hydrophilic nature of the CN particles such that it can be properly dispersed into an epoxy resin. However, each of these solutions are not scalable for high-volume applications, and thus limits CN capability for industrial use.

One promising approach to manufacturing composites with enhanced mechanical properties via complete CNC dispersion is to disperse the CNC into the epoxy resin prior

to impregnating the glass fibers, such that the homogeneously dispersed CN yield a polymer matrix with increased mechanical properties [37]. Although CNC are hydrophilic and tend to agglomerate within the epoxy resin, there may be an intermediate step within the making of the epoxy resin such that incorporating the CNC may be easily facilitated.

An alternative solution to incorporating CNC into glass fiber/epoxy composites has been to coat the glass fibers with the nanomaterials prior to making the composite. Increased mechanical properties as a result are observed due to the increase in the interfacial shear strength and bonding between the glass fibers and the epoxy matrix. The mechanism in which the CNC are bonded to the glass fibers is by hydrostatic forces. Chen et al. [38] had deposited bacterial cellulose (BC) onto the surface of glass fibers during the process of fermentation. The BC coated GF were subsequently mixed into epoxy, where the increase in interfacial shear strength observed was due to an increase in interfacial surface roughness, and the chemical bonding between the BC coating and the epoxy matrix. However, for industrial application, growing BC on the surface of GF is impractical. Additional work and studies must be completed to find a process that makes coating glass fibers quick, inexpensive, and efficient. In addition, more work must be done to link changes in interfacial shear strength due to CNC coating to macroscopic mechanical properties within composites.

Based on the summary of the possible methods that have been used to add CNC into epoxy resins provided above, the following two methods are employed in this study. In the first one, the CNC are added in the epoxy resin and in the second they are added as a coating onto the glass fibers.

First method: The amount of CNC to be used was determined based on the needed viscosity such that it can be seamlessly used within the SMC machine. The hardener and epoxy resin were mixed at a 2:1 ratio. It is noted that the curing process is initiated and completed within 3 hours of the mixing. Freeze-dried CNC is dispersed into the hardener/filler mixture via sonication. Since no monomer has been added to this mixture, sonication can facilitate mixing at elevated temperatures with less viscous resistance, since the curing process is not initiated until the monomer is mixed into the mixture. This method could possibly allow the CNC to be fully mechanically mixed with minimal agglomeration within the epoxy resin, and is worth exploring within this study. With this method, the CNC would serve as an auxiliary reinforcement to the epoxy resin, thus providing increased mechanical properties as desired.

Second method: An aqueous solution of CNC is prepared by diluting an 11.5 wt% suspension of CNC with deionized water. Once the glass fibers are fully immersed within the CNC bath, they are removed and the CNC are allowed to dry on the glass fibers. Finally, the CNC-coated and dried glass fibers are chopped and impregnated by the epoxy resin. This coating process can be easily scaled up and integrated with the SMC manufacturing line. This process could provide an enhanced GF/epoxy interface such that loads could be easily distributed from the epoxy matrix to the glass fibers such as to provide increased reinforcement and thus, increased mechanical properties. The CNC dispersion issue is not a concern in this approach as CNC are already distributed by the glass fibers into the composite.

To the best of the author's knowledge, no study currently exists that bridges the use of nanocomposites with industrial scale manufacturing of automotive components.

The goal of this study is to identify a process that can utilize renewable sources of nanoparticles within conventional industrial composite manufacturing lines, where less heavy components (i.e., glass fibers) may be replaced with lighter components (i.e., nanoparticles) such that the resulting composites are lighter without sacrificing the mechanical properties of the composite and this process can be utilized at an industrial scale for incorporation and utilization within the automotive industry.

2.2 Calibration of the SMC manufacturing line

Sheet-molding compounds (SMC) are thin sheets of fibers pre-compounded with a thermoset resin and are used primarily in compression molding process [30]. Common resins used currently for SMC are polyesters and vinyl esters. Epoxies currently have limited use within SMC due to its longer cure times. There are currently three types of sheet-molding compounds used in industry today: SMC-R, SMC-CR, and XMC [30]. SMC-R refers to randomly oriented, discontinuous fibers. This type of sheet-molding compound is usually denoted with the fiber content, i.e., SMC-R30, indicating 30 wt% GF. SMC-CR refers to sheet molding compounds with a layer of continuous, unidirectional fibers on top of a layer of discontinuous random fibers. This may also be denoted by the fiber content for each layer (i.e., SMC-C40R30). Finally, XMC refers to sheet molding compound that has continuous fibers oriented in an X-pattern over randomly distributed fibers, usually at an angle of 5º-7º.

In addition to the fibers and the resin, several external materials are used within SMC such as to ensure proper manufacturing of the composites. Catalysts (also called initiators) are used to initiate the polymerization process at a particular instance. Inhibitors are utilized to prevent premature curing (gelation) within the sheets. Mold

release agents acts as a lubricant to facilitate easy removal of the composite from the mold (carrier film). Finally, thickeners (also called fillers) are used within SMC to increase the viscosity of the resin such that it can be easily handled by the SMC machine. Thickeners must be used at a proper ratio to ensure that the resin may pass through the machine, but also such that the resin will fully wet-out the distributed fibers.

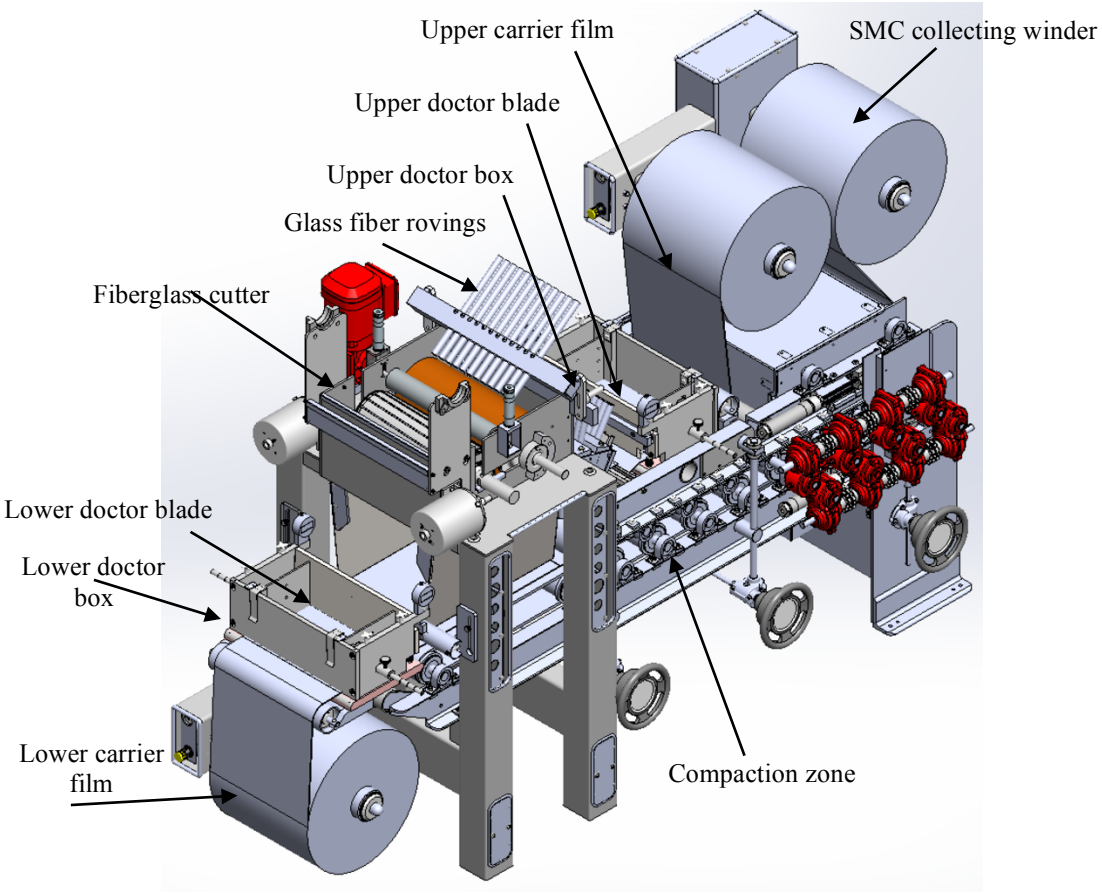

Figure 2.1: Schematic of Sheet Molding Compound (SMC) Line used in this research

As described earlier, sheet molding compounds are made by a process impregnating fibrous materials between two layers of a thermosetting resin, and then allowing these layers to be compacted into composite sheets, which are then collected and stored/conditioned. This process has been the primary manufacturing method for

glass fiber-based composites due to its high-volume capability, efficiency, part reproducibility, and surface finish. The diagram for the SMC machine used in this study is shown in Figure 2.1.

As shown in the figure, GF rovings are pulled into the machine, in which they are subsequently cut to a set length (25.4 mm) and allowed to be deposited randomly onto the resin below supported by carrier film, usually made of polyethylene. As the glass fibers fall onto the lower resin layer, the two layers are then met by the upper resin layer and carried into the compaction zone. As the layers pass through the set of compaction rollers, the trapped air is removed and the glass fibers are fully wetted by the resin. The amount of resin for each layer is controlled by the width of the doctor box walls and the vertical doctor blade height (opening). The amount of fibers deposited per unit length is controlled by the cutting speed specified on the machine as well as the conveyor speed. The final composite sheet exits the machine, and is collected on a collector roll to be further processed. This process would be run until all of the resin for the individual run has been consumed.

To effectively measure and characterize the properties of the composite made by the SMC, complete control of the SMC production line had to be established. In other words, the inputs of the SMC had to be calibrated such that we can accurately produce a desired output. Processing parameters of the SMC included conveyor speed, cutting speed, blade height, and box width, much like the industrial-scale SMC. Specifically, conveyor speed and cutting speed characterized the weight of the fiber per unit area, and the blade height and box width characterized the weight of the resin per unit area. Once

these weights were determined, the composition of the output composite could be determined for further reference.

For this study, composites were made with a fiber loading of 30% GF (SMC-R30). In order to achieve composites with this specific fiber loading, two calibration processes were been implemented on the SMC machine, one for the fiber loading, and another for the resin content. For the fiber loading, first the speed of conveyor (cm/s) was determined from the conveyor control reading of the display. A set length was marked on the carrier film of the machine, and multiple runs would be made at a specific conveyor reading and the time for that length to be traversed would be recorded. This was to determine the speed of the conveyor for each reading. A graph of the conveyor calibration is shown in Figure 2.2.

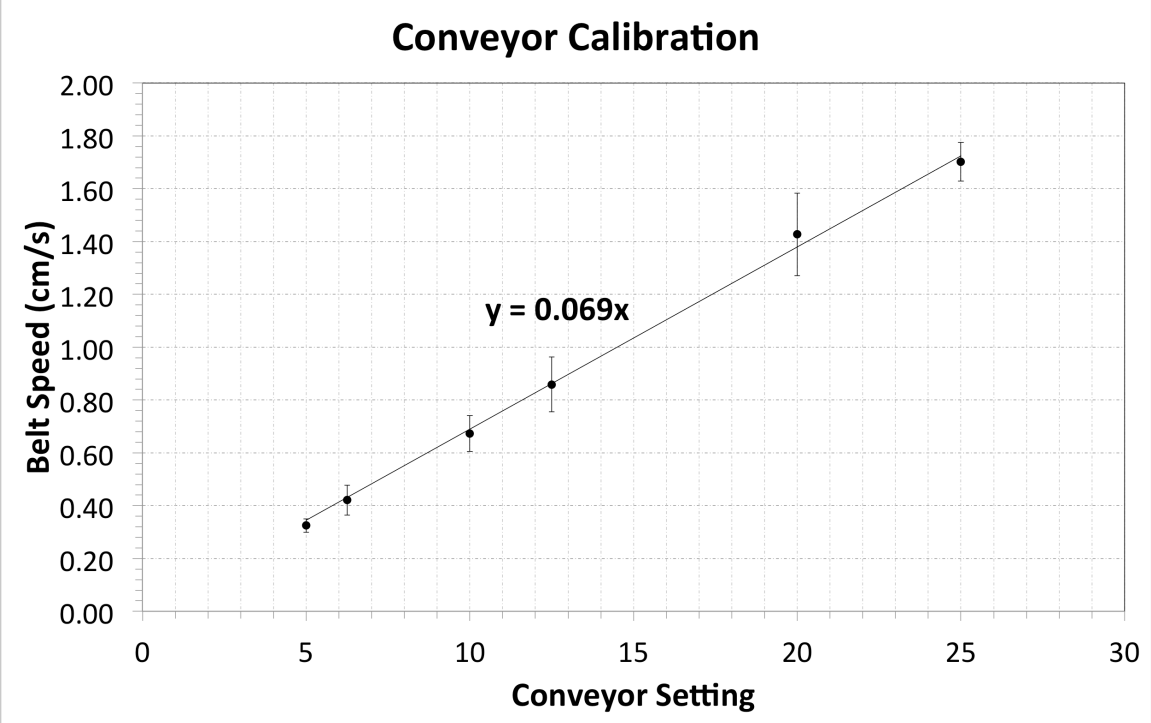

Figure 2.2: Conveyor Belt Speed Calibration

Secondly, the mass per unit time (g/cm-s) was determined from the cutting control reading for one roving. This calibration was applied to multiple rovings under the

assumption that each roving would be spaced 1 inch apart from another roving. The blade would be run at a specific cutting speed for a set amount of time, and the cut fibers from that run was collected and weighed. A graph of the cutting calibration for multiple cutting speeds is shown in Figure 2.3.

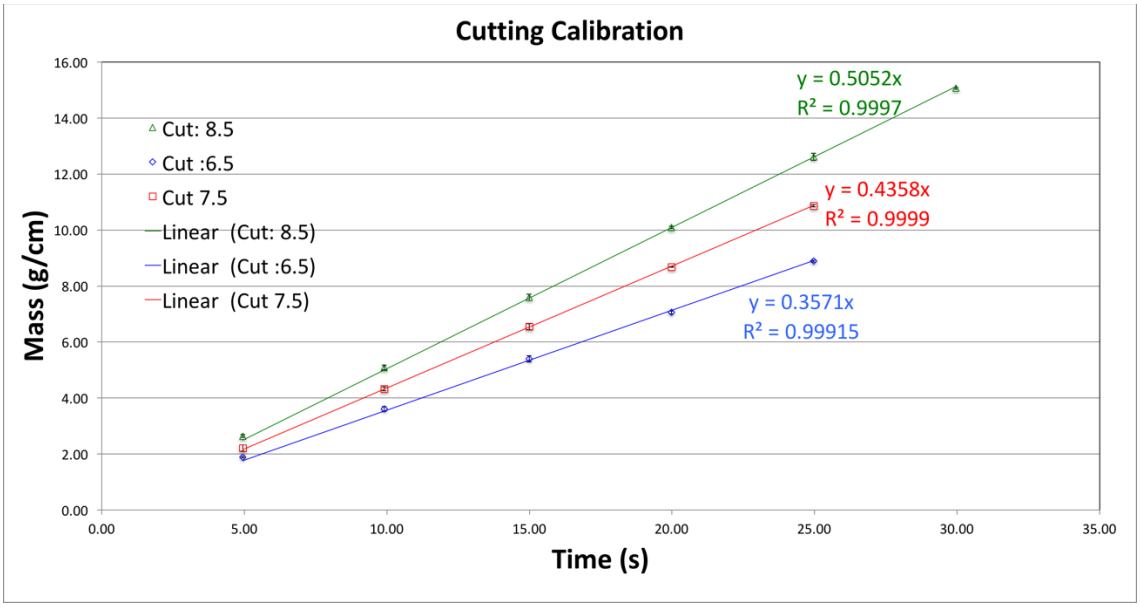

Figure 2.3: Cutting Speed Calibration

The slope of each curve gives the mass per unit time needed to determine the mass of the fiber deposited per unit area (g/cm^2) for a specific cutting speed and conveyor speed. A graph of the final calibration curves for three different cutting settings is shown in Figure 2.4.

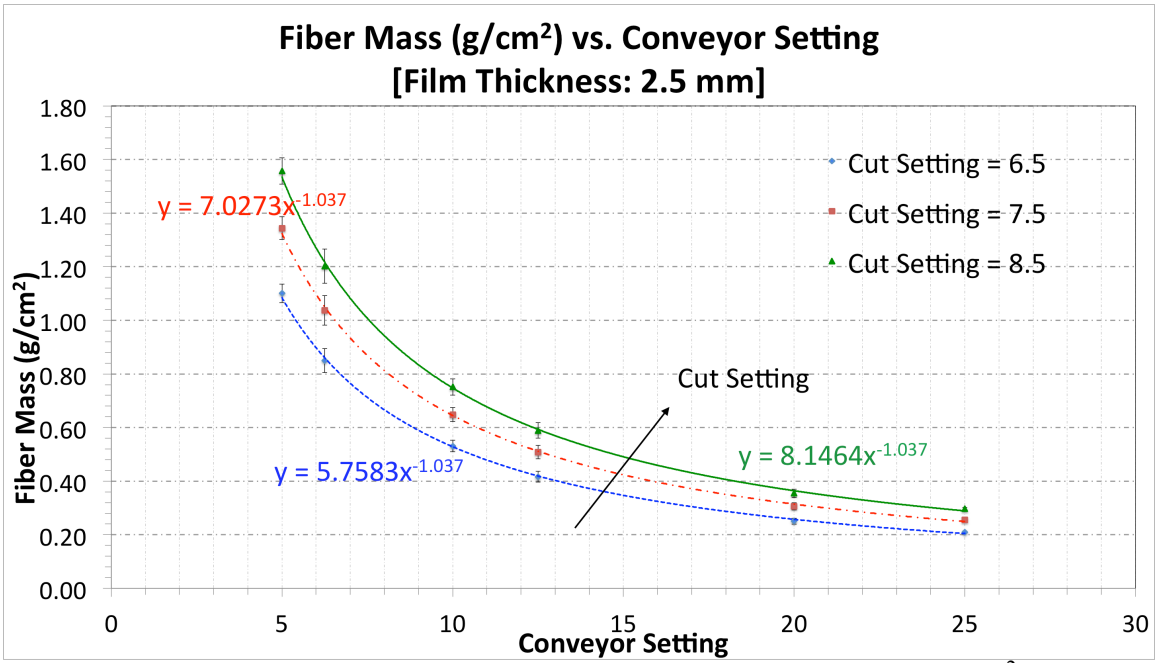

Figure 2.4: SMC Calibration (Conveyor Setting vs. Fiber mass (g/cm^2))

Next, the amount of resin controlled by the doctor blade had to be determined from the desired final dimensions of the composite (11 in wide x 2.5 mm thick). To determine the initial dimensions of the doctor box width and height, the spreading ratio had to be determined for the compression settings used in the SMC. This is done by measuring the width and thickness of the initial resin sheet, and, after compaction, measuring the width and thickness of the final sheet to determine the spreading ratio. For the compaction settings used in the study, this ratio was found to be 0.72. From this ratio, the initial doctor box width was found to be 201 mm, and the initial doctor box height was found to be 3.46 mm. Given the density of the resin to be 18.55 g/cm^3, the mass of the resin per unit area was found to be 0.28 g/cm^2. This was compared to the fiber mass per unit area calculated earlier for to determine the optimal conveyor and cutting settings to achieve a 30 wt% fiber loading. From the calibration curves, the optimal conveyor setting was found to be 20.0 with a cut setting of 6.5, and, by halving the fiber content, a

30 wt% loading can be achieved. A table of the fiber content as a function of the conveyor setting is shown in Tables 2.1-2.5.

Table 2.1: Material Properties

Material Properties					
	Mass Fraction (%)	Volume Fraction (%)	Density (g/cm^3)	Density (g/in^3)	Spreading Ratio (wi/wf)
Royce International Epoxy 928	0.75	0.73	1.16	18.98	
Royce Curing Agent 9908	0.25	0.27	1.06	17.40	
Combined Resin	1.00	1.00	1.13	18.55	0.72

Table 2.2: SMC Sheet Settings (30 wt%)

SMC Sheet Settings (30% wt.)				
Final Width (in)	Final Thickness (mm)	Initial Width (in)	Initial Thickness(mm)	Weight (g/cm^2)
11.00	2.50	7.94	3.46	0.28

Table 2.3: Composite Composition (Cutting Speed: 8.5)

Composite Properties	**2.5mm x 11 in**	**Cut = 8.5**			
Conveyor Setting	Fiber (g/cm^2)	Resin (g/cm^2)	Total Mass	Fiber %	Resin%
5.00	1.54	0.28	1.82	0.84	0.16
6.25	1.22	0.28	1.50	0.81	0.19
10.00	0.75	0.28	1.03	0.73	0.27
12.50	0.59	0.28	0.88	0.68	0.32
20.00	0.36	0.28	0.65	0.56	0.44
25.00	0.29	0.28	0.57	0.51	0.49
30.00	0.24	0.28	0.52	0.46	0.54
35.00	0.20	0.28	0.49	0.42	0.58
40.00	0.18	0.28	0.46	0.39	0.61

Table 2.4: Composite Composition (Cutting Speed: 7.5)

Composite Properties	**2.5mm x 11 in**	**Cut = 7.5**			
Conveyor Setting	Fiber (g/cm^2)	Resin (g/cm^2)	Total Mass	Fiber %	Resin%
5.00	1.32	0.28	1.61	0.82	0.18
6.25	1.05	0.28	1.33	0.79	0.21
10.00	0.65	0.28	0.93	0.70	0.30
12.50	0.51	0.28	0.80	0.64	0.36
20.00	0.31	0.28	0.60	0.53	0.47
25.00	0.25	0.28	0.53	0.47	0.53
30.00	0.21	0.28	0.49	0.42	0.58
35.00	0.18	0.28	0.46	0.38	0.62
40.00	0.15	0.28	0.44	0.35	0.65

Table 2.5: Composite Composition (Cutting Speed: 6.5)

Composite Properties	**2.5mm x 11 in**	**Cut = 6.5**			
Conveyor Setting	Fiber (g/cm^2)	Resin (g/cm^2)	Total Mass	Fiber %	Resin%
5.00	1.09	0.28	1.37	0.79	0.21
6.25	0.87	0.28	1.15	0.75	0.25
10.00	0.53	0.28	0.81	0.65	0.35
12.50	0.42	0.28	0.70	0.60	0.40
20.00	0.26	0.28	0.54	0.48	0.52
25.00	0.21	0.28	0.49	0.42	0.58
30.00	0.17	0.28	0.45	0.38	0.62
35.00	0.14	0.28	0.43	0.34	0.66
40.00	0.13	0.28	0.41	0.31	0.69
55.00	0.09	0.28	0.37	0.24	0.76

After being calibrated to quantitatively produce the correct composite, several defects still have to be addressed in order to ensure that a testable composite was being produced. The first issue is that of "resin pockets," in which there would be areas in the film which there are no fibers present. These resin pockets introduce stress-concentration

areas that possibly could decrease the overall mechanical properties of the composite. This issue has to be resolved by adjustment of the cut fibers, by determining which rovings would be cut, and by placement of these rovings over the carrier film, such that they are distributed evenly and randomly. Secondly, the issue of unwetted fibers must be addressed. This issue suggests that the fibers are not distributed evenly onto the carrier film, and the plates produced would not be representative of the desired composite (i.e., 30 wt% GF). This may be caused by insufficient compression, low resin content, or uneven distribution of fibers. To address this issue, the fibers must be properly aligned within the resin layer, and the compression settings must be adjusted accordingly such that there is a uniform spreading throughout the carrier film. The issue of resin extraction is last, in which the final composite would exceed the dimensions of the carrier film, and after compression, would be extracted outside of the film and onto the SMC machine. Ultimately this is a waste of material, and also may suggest that the composite in the film is not uniform. This issue suggests that too much pressure was applied in the compaction zone, the resin and fibers were not properly aligned on the carrier film, or too much material was being used in an individual run. To accommodate for this, proper adjustment of the doctor box must be implemented and adjustment of the cut rovings, specific amounts of material must be applied at once, and the compaction settings must be adjusted accordingly.

CHAPTER 3

LAB SCALE STUDIES: IMPROVING THE INTERFACIAL SHEAR STRENGTH

An increase in the mechanical properties of the GF-epoxy composite can be attributed to an increase in the interfacial shear strength between the epoxy resin and the glass fibers. One method for increasing the interfacial shear strength is by coating the glass fibers with cellulose nano-crystals such that the mechanism in which a load is transferred from the epoxy to the glass fiber is enhanced. To determine if a coating method is feasible for increasing the bond between glass fibers and the epoxy matrix, a lab-scale study was performed to analyze the effect different coating conditions have on increasing the interfacial shear strength using single fiber fragmentation tests, and to determine the optimal coating consistency such that the interfacial shear strength is maximized. In addition to this study, composites were made using lab-scale fabrication methods to validate the hypothesis that increase in interfacial shear strength results in enhancement of the composites' macro-mechanical properties.

3.1 Experimental Details

3.1.1 Materials

Optimizing the interfacial shear strength between glass fibers and epoxies that would be used in the automotive and marine industries requires the appropriate materials. Owens Corning (Oak Brook, IL, US) ME1510 multi-end roving GF (single filament diameter of 10±1 μm) were used as received since it is sized specifically for Epoxy-based SMC. It utilizes Advantex GF which is calcium aluminosilicate glass that provides the mechanical properties of E-glass with the acid corrosion resistance of E-CR glass.

Mechanical properties presented in this study further improve upon the characteristics of composites using this specific glass fiber. The GF rovings were chopped to an average length of 25±0.5 mm.

A bicomponent epoxy resin consisting of 635 thin epoxy and 556 slow amine hardener supplied by US Composites (Wes Palm Beach, FL) was used. CNC in the form of 11.9 wt% never-dried suspension in water [39] was supplied by the USDA Forest Service-Forest Products Laboratory (FPL), Madison, WI, USA. The average length and width of the CNC were 6.4 ± 0.6 and 138 ± 22 nm, respectively [40].

3.1.2 Coating of GF with CNC

CNC coated GF were produced by immersing ~ 154 g of chopped GF rovings in ~1000 ml of aqueous CNC suspension without agitation for 2 min, after which the GF were taken out and spread on covered trays with ample ventilation to dry 24 h at room temperature. This simple, low cost coating method is conceptually scalable for larger volume applications. The CNC used were not functionalized or surface treated. For uncoated GF, a similar procedure was followed using distilled water with no CNC to maintain the consistency in fabrication. The CNC suspension was diluted, in order to adjust the CNC coating, using distilled water and then sonicated to achieve a uniform CNC dispersion in water. Sonication was carried out using Misonix S-4000 ultrasonic processor equipped with a 12.5 mm probe diameter at 30% amplitude and 20 W power for 8 min. Aqueous CNC suspensions of 0, 0.5, 1, 1.5, 2, 3 and 5 wt%, were prepared using the above procedure and used to coat the chopped GF rovings. The corresponding naming scheme used to describe the coated fibers is as follows: GF, 0.5S-GF, 1S-GF,

1.5S-GF, 2S-GF, 3S-GF, and 5S-GF, respectively. The "S" in this case represents CNC suspension.

3.1.3 SFFT Sample Preparation

For SFFT specimen preparation, a single GF was placed in the middle of a dogbone shaped mold and covered with epoxy resin that was cured at 80 °C for 1 h, followed by post-curing at 100 °C for 4 h. The resin was prepared by mixing the epoxy with hardener at 2:1 wt% using a VWR magnetic stirring plate at 60 rpm, at room temperature for 10 min, and was degassed in a vacuum chamber for 10 min prior to pouring into the mold. SFFT specimens were prepared using the following naming scheme: GF, 0.5S-GF, 1S-GF, 1.5S-GF, 2S-GF, 3S-GF, and 5S-GF. Note that to obtain single GF, individual fibers were carefully pulled off from the coated and uncoated GF rovings. The SFFT dogbone specimens were made according to the test protocol for SFFT [41].

3.1.4 Fabrication of CNC-coated GF/epoxy Composites

GF/epoxy composites were produced with a 30 wt% GF content. Chopped GF rovings with or without CNC coatings were added and mixed with the resin using a spatula and degassed in a vacuum chamber, for 10 min. Then, the mixture was spread in a rectangular mold and cured as described above for the SFFT samples. Based on the SFFT results (see section 2.2.2), only 1S-GF, 1.5S-GF and 2S-GF were used to make CNC-GF/epoxy composites. The naming scheme used in the paper for the GF/epoxy composites is as follows, GF/epoxy (uncoated GF) and αCNC-βGF/epoxy, where α is the CNC wt% content on the GF, as estimated on TGA analysis (see section 2.2.3) and β is the GF wt% in the composite. The test coupons were cut from the plate using a waterjet cutter (MAXIEM 1515).

3.1.5 Characterization Techniques

SFFT tests, as described by Hunston et al. [41], were used to quantify the effect of CNC coatings on the IFSS. In brief, tensile tests, with applied load along the fiber axis direction, were carried out at a displacement rate of 1 mm/min using an Instron 33R 4466 equipped with a 500 N load cell. The tests continued until the load dropped at 90-95% of maximum load to ensure that no further fiber fragmentation could occur. The IFSS was determined by Kelley and Tyson model [42] given in Eq. (1),

$$\tau_i = \frac{d_f \sigma_f}{2 l_c} = \frac{3 d_f \sigma_f}{8 \bar{l}} \qquad (1)$$

where τ_i is the IFSS, d_f is the fiber diameter, l_c is the fiber critical fragmentation length, $\bar{l}$ is the average length of fiber fragmentation segments (l_c=4$\bar{l}$/3), and σ_f is the fiber strength. The fiber diameter and fiber fragmentation lengths were measured using polarized microscopy. The GF strength was estimated by tensile testing (ASTM D3822), where a single GF was attached to a paper tab and tested at a displacement rate of 1 mm/min using the Instron. An average GF strength of 2800±o350 MPa was measured, and as expected, the CNC coating process did not affect the single GF ultimate strength. Both the strength value and the IFSS values reported are an average of at least 10 measurements.

A Leica DM2500 polarized light optical microscope was used to characterize CNC coatings on chopped GF rovings, and to measure the fiber fragmentation lengths in SFF tests. A Hitachi SU 8230 field emission scanning electron microscope (FE-SEM) at an acceleration of 5 kV were used to view the CNC coatings on individual GF, and the

fracture surfaces of the composites. A plasma sputter (Ted Pella Inc.) was used to apply gold coating on the surface of the samples prior to SEM imaging to minimize charging.

Water displacement method was used to measure the specific density of the composites according to ASTM D-792. Thermo-gravimetric analysis (TGA), using TGA SDT Q600 (TA Instruments), was used to assess the thermal stability of CNC and determine the CNC content on the GF. The samples were heated from 50 °C to 500 °C at 10 °C/min in inert atmosphere. Each data point is an average of at least 3 measurements.

The tensile properties of the composites were determined according to ASTM D638 using an Instron 33R 4466 equipped with 10 kN load cell. An extensometer, Instron 2630-35, with a gauge length of 50.8 mm was used. The modulus was calculated between the axial strain values of 0.05% and 0.2%. Each tensile data point is an average of at least five samples. The flexural properties were measured using three-point bending tests with an Instron 33R 4466 equipped with 10 kN load cell according to ASTM D790-02 with a support span of 50 mm and thickness of 5 mm at a displacement rate of 0.85 mm/min. Each flexural data point is an average of at least seven tests. Dynamic mechanical thermal analyses (DMA Q800, TA Instruments) in three-point bending mode was used to measure the storage and loss moduli and the glass transition temperature (T_g) in the 25 °C −160 °C range at a heating rate of 5 °C /min and 1 Hz. A preload of 0.01 N and a maximum strain of 0.05% were applied on the specimens. Each data point is an average of at least five tests.

3.2 Results

In order to test the hypothesis that addition of CNC on the GF/epoxy interface can improve the mechanical properties of the composites, composites with uncoated and

CNC coated GF were compared in terms of mechanical properties. First, it was determined whether or not the CNC alter the GF/epoxy interface and the optimum CNC concentration needed to increase the properties of the composites with no cost and weight penalty.

3.2.1 CNC coatings on GF

GF rovings were coated with CNC according to the process described previously. As shown in Figure 3.1 (a) − (b), a thin layer of CNC is deposited on the GF surface as a result of physical absorption (e.g., hydrogen bonding of the accessible –OH side groups on the CNC surface as described in Chen et al. [38]). Of interest is how the CNC coated the chopped GF rovings, as well as individual GF within the rovings. To observe the surface of individual GF, the GF were pulled out from the chopped GF rovings after the coating process. As shown in Figure. 3.1 (c) − (e), the uncoated GF has a smooth surface, while the surface of CNC coated GF is rougher, indicating that CNC have been deposited on the GF surface. Additionally, the coated GF surface roughness appears to increase with the CNC coating deposition concentration, suggesting that more CNC are deposited on the GF surface. Some of the roughness features in the CNC coating on individual GF is likely associated with the CNC coating process using the GF rovings as opposed to individual GF, in which GF-GF meniscus formation within GF rovings during drying would cause deposition variations. In addition, deformation of the CNC coating would occur when separating GF from other GF within the GF roving.

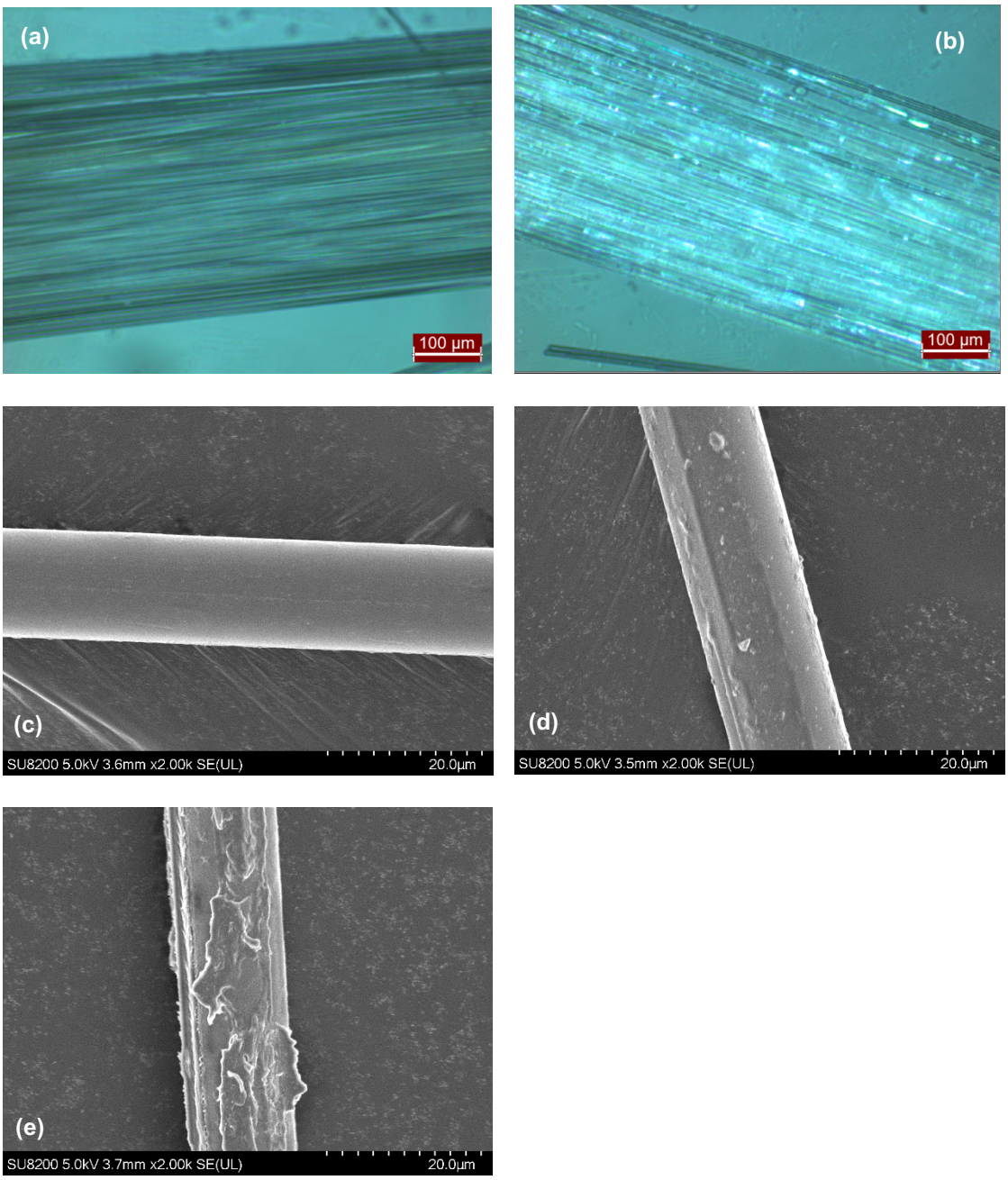

Figure 3.1: Polarized micrographs (polarized light of 95°) of chopped GF rovings, (a) uncoated, and (b) coated 1.5S-GF; SEM images of single GF coated with CNC (c) 0 wt%, (d) 1 wt % and (e) 5 wt% suspensions

The implications of these observations are that, although GF rovings are used in the coating process, the CNC suspension can penetrate the GF rovings and coat individual GF. The differences in the GF surface roughness of individual GF may subsequently alter the stress transfer efficiency at the GF/epoxy interface in SFF testing that uses individual GF, as seen in Section 3.2.2.

3.2.2 Interfacial properties

Figure 3.2(a) shows an optical image of a post-tested SFF 0.5S-GF test coupon with three fracture events along the GF, where the distance between each fracture represents an individual fiber fragment length. The average fiber critical length (= $4\bar{l}/3$, where $\bar{l}$ is the average of several individual fiber fragment lengths), and the calculated IFSS, as a function of CNC coating concentration on the GF surface, are shown in Figure 3.2(b).

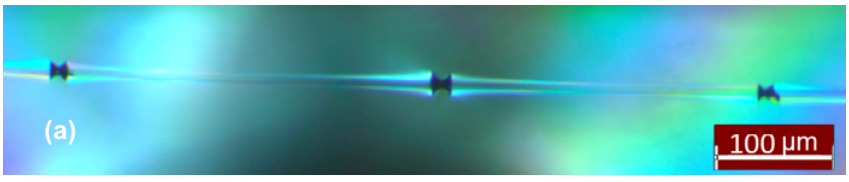

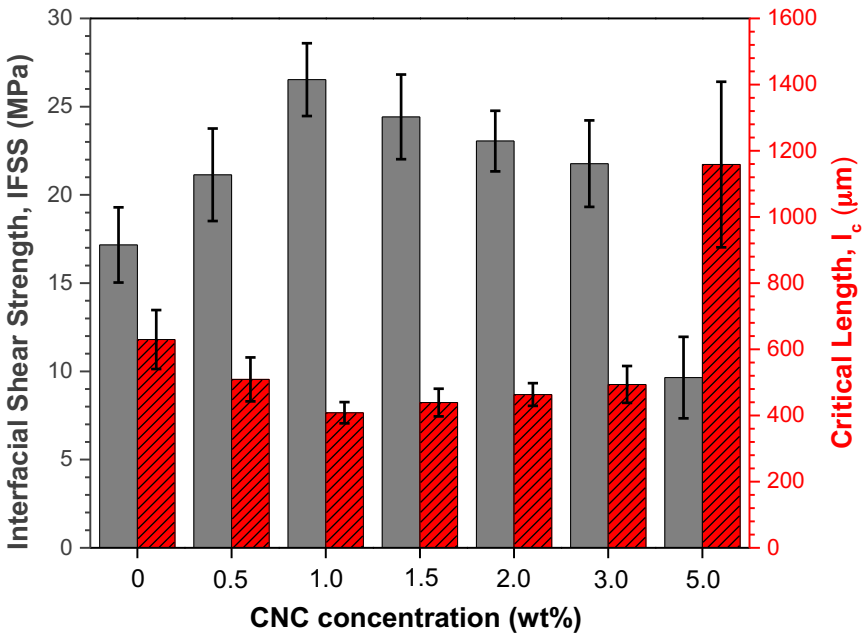

Figure 3.2: SFF results: (a) Polarized light micrograph of a single GF coated with 0.5CNC-GF (polarized light 80°) embedded in epoxy showing representative critical fragmentation length, (b) Interfacial shear strength (solid gray bars) and critical fragmentation length (striped red bars) for composites as a function of CNC suspension concentration. Error bars are one standard deviation.

Changes in both the IFSS and fiber critical length when the GF are coated indicate that the load transfer across the GF/CNC/epoxy interface has been modified. Possible mechanisms are mechanical interlocking between the GF and epoxy due to the increased GF surface roughness and corresponding increased surface area, as well as hydrogen bonding between hydroxyl containing CNC and epoxide groups in the epoxy. There appears to be an optimum condition, i.e., 1S-GF for which the IFSS reaches a maximum, that corresponds to ~60 % increase compared to that of the uncoated GF/epoxy specimen. As the concentration of CNC suspension increases, i.e., for 1.5S-GF, 2S-GF, 3S-GF, and

5S-GF SFF cases, there is a reduction in IFSS. The lower IFSS suggest that the CNC coatings have reduced the stress transfer efficiency at the GF/CNC/epoxy interface. A few mechanisms are plausible, which can be based on the quality of the CNC coating and associated interfacial defects. As shown in Figure 3.2(e), 5S-GF tend to have rougher surfaces and other defects within the CNC coating, e.g., formation of CNC multilayer that can potentially result in slippage of CNC with respect to each other and reduction of the stress transfer efficiency.

There were various fracture modes observed for the specimens with different CNC coating contents, suggesting that there is a change in the interfacial properties at the GF-epoxy interface caused by the CNC coatings, as depicted in Figure 3.3.

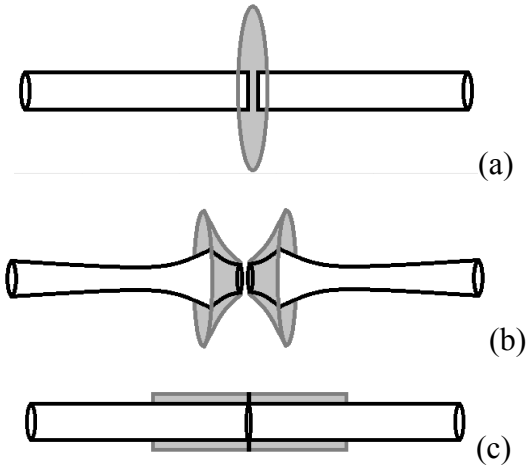

Figure 3.3 Three modes of fracture in matrix in single fiber fragmentation test; (a) *Mode i:* disk-shaped fracture of matrix referring to strong interface, (b) *Mode ii:* double-cone matrix fracture suggesting a matrix with a low shear strength, and (c) *Mode iii:* debonding of fiber and matrix inferring a weak interface

According to Mullin et al. [43], fracture modes in single fiber fragmentation tests can be categorized to three modes based on the fiber/matrix level of adhesion; *mode i*:

following the fiber break, a disk shaped matrix crack occurs as a result of normal stresses, shown in Figure 3.3 (a), suggesting a strong interface; *mode ii*: following the fiber break, a double cone-shaped matrix crack with 45° angle occurs as a result of shear stresses, shown in Figure 3.3 (b), referring to a type of interface in which the matrix shear strength is lower than its tensile strength ; and *mode iii*: fiber break is instantly followed by a limited interfacial debonding due to shear stress, shown in Fig. 3.3(c), implying a weak interface type. The debonded interface cannot transfer any load from matrix to the fiber and the length of deboning can be used as an indicator of fiber stress and interfacial energy [44]. For epoxies, concurrent disk-shaped and cone-shaped matrix cracks formed at the fiber ends are commonly seen. In the current study, combined fracture modes *i* and *ii* along with few cracks of mode *iii* were observed for the GF and 0.5S-GF samples, as shown in Fig. 3.4 (a) − (c). The fracture mode for 1S-GF, 1.5S-GF, 2-S-GF, and 3S-GF SFF samples were combined modes *i* and *ii*, shown in Fig. 3.4 (d) − (e), suggesting a stronger interfacial bonding compared to uncoated-GF/epoxy samples. The fracture modes for 5S-GF samples were mode *ii* and mode *iii*; however, it was observed that the debonded areas increased compared to that of uncoated GF/epoxy samples implying a weaker interface and a lower IFSS value, as seen in Figure 3.2.

(a) 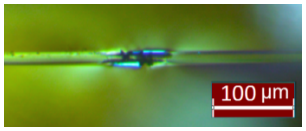

(b)

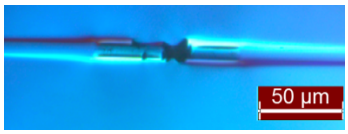

(c)

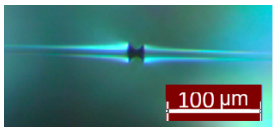

(d)

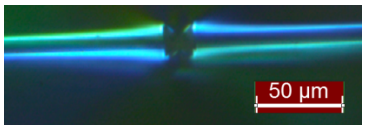

(e)

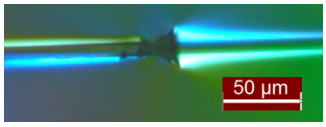

Figure 3.4: Optical polarized light micrographs of SFF specimens after tensile test showing fracture events at the GF: (a) GF/epoxy (polarized light of 75°), (b) 0.5S-GF (polarized light 120°), (c) 0.5S-GF (polarized light 80°), (d) 1S-GF (polarized light 90) and (e) 2S-GF (polarized light 75°)

3.2.3 Specific density, CNC content and thermal stability

GF/epoxy composites were made using the following chopped GF rovings: GF, 0.5S-GF, 1S-GF, 1.5S-GF and 2S-GF. The density for all these composites was found to be 1.3 ±0.03 g/cm^3, delineating that the CNC coatings did not significantly increase the composite weight and is consistent with the small CNC wt% deposited on the GF.

The CNC wt% within chopped GF rovings, as well as within the composites, were correlated with the CNC suspension concentration used in the coating process as shown in Figure 3.5. The uncoated GF used as the baseline for determining the CNC wt% on the coated GF. It is noted that the CNC wt% on the GF surface is not increasing linear with the CNC suspension concentration. The thermal stability of the CNC-coated GF is

also plotted in Figure 3.5. The onset temperature of thermal degradation of the neat CNC was 234.23±0.67 °C. All the coated-GF degraded above this temperature. The onset temperature of thermal degradation decreased with the increase in the CNC content on the GF as it was expected.

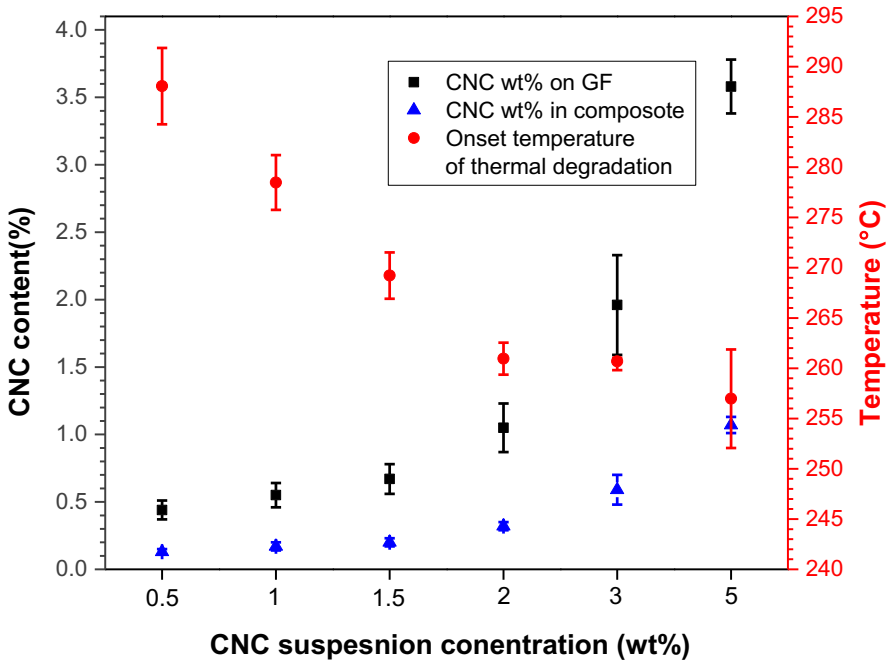

Figure 3.5: CNC suspension concentration on the GFs and composites and onset temperature of thermal degradation for CNC-coated GFs as a function of CNC concentration in the aqueous solution. Error bars are 1 standard deviation.

3.2.4 Fracture surface morphology

The fracture surface of the composites failed in the tensile testing was studied using a FE-SEM. As shown in Figure 3.6 (a) − (b) the main failure mechanism for

uncoated GF epoxy composites was interfacial debonding as indicated by the clean fiber pull-outs devoid of the matrix, indicating weak fiber-matrix adhesion. In contrast, the failure mechanisms for CNC-coated GF epoxy composites were concurrent matrix cracking, fiber breakage and interfacial debonding, shown in Figure 3.6 (c) − (d), implying an improvement in the interfacial bonding as a result of CNC coating. Also, matrix residues on the pulled-out fibers (Fig. 3.6 (d)) and a rough fracture surface for both 1S-30GF/epoxy and 2S-30GF/epoxy composites compared to the smooth fracture surface for the uncoated GF/epoxy composites suggest a better adhesion between fiber and matrix.

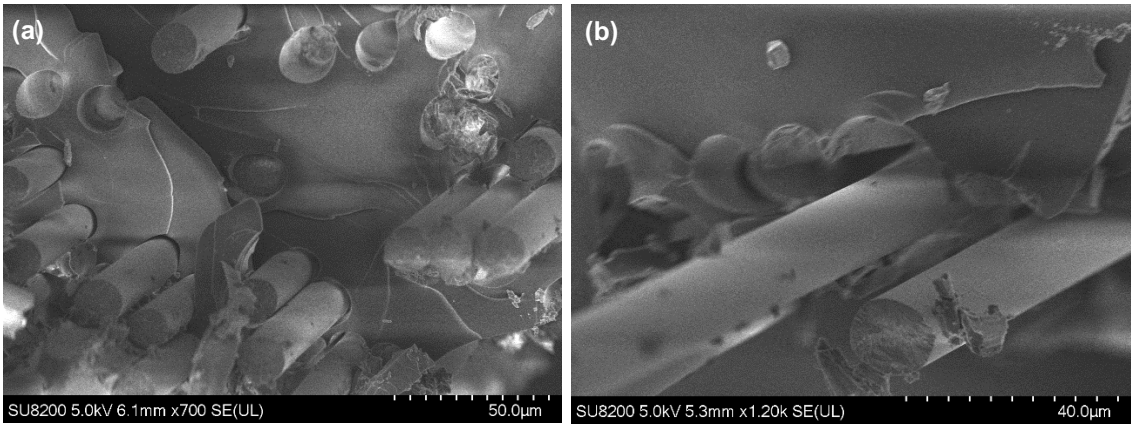

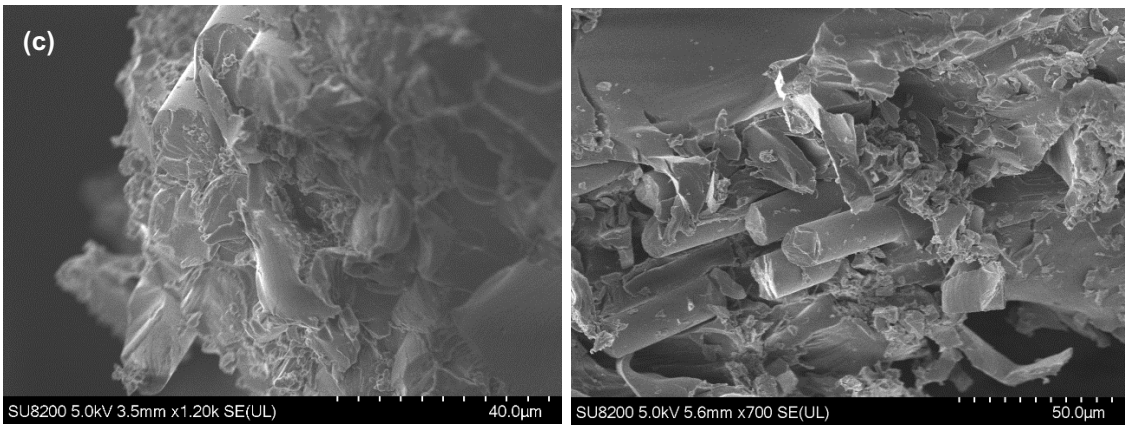

Figure 3.6: SEM images for fracture surface of different epoxy composites; (a) and (b) uncoated 30GF/epoxy, (c) 1S-30GF/epoxy, (d) 2S-30GF/epoxy

3.2.5 Tensile and flexural properties

The effect of the CNC content on the tensile properties of CNC coated GF/epoxy composites are plotted in Figure 3.7. The incorporation of CNC as a coating to GF enhances the elastic modulus by ~ 10% for 1S-30GF/epoxy and 1.5S-30GF/epoxy composites with respect to that of uncoated GF/epoxy. This may be a result of the increase in the stiffness of the GF/epoxy interlayer due to presence of CNC as according to Hashin [45], a stiffer interface results in faster stress transfer across the fiber/matrix interface and thus in higher modulus for the composite [46]. Although this hypothesis is not be validated in this study, Gao et al. [47] reported that increase in the apparent modulus of GF/epoxy interface resulted in increase in the composite macroscopic modulus. In addition, the tensile strength increased for 1S-30GF/epoxy (~10%) and 1.5S-30GF/epoxy (~4%) composites with respect to that of 30GF/epoxy composites. This increase reflects the higher IFSS (see Fig. 7) inferring stronger interfacial interactions and better stress transfer across the fiber/CNC/epoxy interface as reported also elsewhere [48]. The tensile strength of the 2S-30GF/epoxy composite was ~12% lower despite

having higher IFSS compared to that of 30GF/epoxy. This may be due to various mechanisms including void formation within and around the GF rovings as a result of incomplete infiltration of the epoxy with the coated GF rovings and breaking of the CNC coating as it becomes more brittle with increase of its thickness. The strain at break had a trend similar to that of the strength, where the strain at break in 1S-30GF/epoxy and 1.5S-30GF/epoxy composites increased by ~14 % and ~10% while that of 2S-30GF/epoxy decreased compared to uncoated 30GF/epoxy composites.

The effect of the CNC content on the flexural properties of CNC coated GF/epoxy composites are also shown in Figure 3.7. For composites made with 1S-GF and 1.5S-GF, the flexural modulus and strength increased by ~40% and ~42%, respectively, with respect to those of uncoated 30GF/epoxy composites indicating better adhesion between the glass fiber and epoxy due to higher IFSS, and stress transfer at a faster rate as discussed above. The strain at break follows a similar trend to that of axial strain, where it increased by ~10% for 1S-30GF/epoxy. It is noted that the enhancement in flexural properties was larger than the enhancement in tensile properties at the same CNC content. This is typical of defect mediate failure as the volume of material under tensile forces is greater in tensile tests, there is a higher probability of larger sized defects to be within the tensile load, and thus failure occurs at lower applied loads.

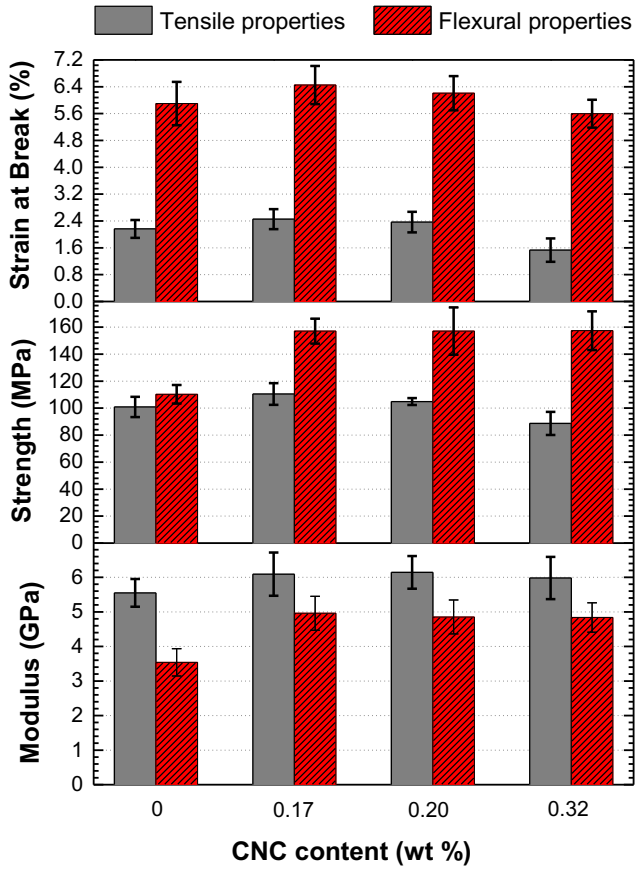

Figure 3.7: Effect of the CNC content (wt% on GF rovings) in CNC-coated 30GF/epoxy composites on tensile and flexural properties. Error bars are 1 standard deviation.

3.2.6 Dynamic mechanical properties

The thermo-mechanical properties of the composites below and above T_g are presented in Table 3.1. At 25 °C, the incorporation of CNC as a coating to GF rovings was shown to enhance the storage modulus (E') for the 1S-30GF/epoxy and 1.5S-30GF/epoxy composites, but the storage modulus for 2S-30GF/epoxy composites was lower as compared to that of 30GF/epoxy composites. The increase in the storage modulus at 25 °C can be attributed to the stiffening of the GF/CNC/matrix interface due to the presence of CNC particles, as discussed in Section 3.2.5. Although the average

value of the rubbery moduli (E_r: the storage modulus above T_g) measured at 90°C for the composites containing CNC-coated GF were lower than that the composite incorporating uncoated GF, due to the large standard deviation in measured properties, it was concluded that coating of the GF with CNC did not impact the rubbery modulus. Studies have shown that addition of CNC in the epoxy increased the rubbery modulus due to the formation of a network of mechanically percolated CNC [16, 18, 21]. However, it is expected that CNC on the surface of the GF do not form a percolated network within the polymer matrix. Hence, CNC cannot strongly impact the polymer chain segmental motion and consequently, the rubbery modulus. Presence of CNC has no effect on the tan δ and the glass transition temperature (T_g).

Table 3.1: Viscoelastic properties of CNC-GF/epoxy composites in three-point bending mode

Composite	E' @ 25 °C (MPa)	E_r @ 90 °C (MPa)	T_g (°C)	tan δ @ Tg
30GF/epoxy	4932±586	250±21	50.3±0.7	0.61±0.06
1S-30GF/epoxy	5213±543	224±31	49.4±0.5	0.61±0.02
1.5S-30GF/epoxy	5614±695	228±22	50.2±0.8	0.65±0.07
2S-30GF/epoxy	4634±257	243±38	49.5±1.1	0.59±0.02

E': storage modulus
E_r: rubbery modulus
T_g: glass transition temperature measured at in tan δ peak
tan δ: value of tan δ peak

3.3 CNC Bath Design, Integration, and Construction

Based on the results of the lab-scale study in which coating the glass fibers was done manually to prove the effect coating has on the macro-mechanical properties of the resulting composite, a mechanism in which glass fibers could be coated and input into the SMC manufacturing line was designed, constructed, and integrated. This mechanism would allow the glass fibers to be immersed in a CNC bath at an optimal residence time, and then given ample time and heat necessary to dry the glass fibers before being input

and cut into the SMC line. This mechanism would prove a useful tool such that industrial composite manufacturers can utilize the CNC coating method to improve the overall quality of the resulting composites, and thus is an attractive project for industrial applications. To successfully design the bath, several factors had to be taken into account such as immersion time, drying time, and design characteristics.

3.3.1 Immersion Time

Before the bath could be constructed, the proper time in which the glass fibers need to be immersed within the CNC bath had to be determined. This study was done by immersing glass fiber rovings into a CNC 1wt% solution for the following residence times: 0s, 2s, 4s, 6s, 8s, and 10s. After the glass fiber rovings were immersed, a sample from each of the residence times were analyzed under an SEM to verify that CNC were deposited onto the glass fibers themselves. Quantitative analysis was done to determine how much CNC was deposited with each residence time. In addition, TGA was performed to determine the quantitative amount of CNC deposited for each residence time. The combination of these results would allow for the successful determination of the optimal immersion time.

Shown in Figures 3.8-3.13 are the SEM images for each of the residence times (i.e., 0s-10s). As shown in each figure, there is a clear increase in CNC deposition as the immersion time increases. The CNC appear as long, thin, rod-like ellipses and also as a coating in each of the SEM images. There also seems to be a more uniform coating for 4s more so than the rest of the immersion times.

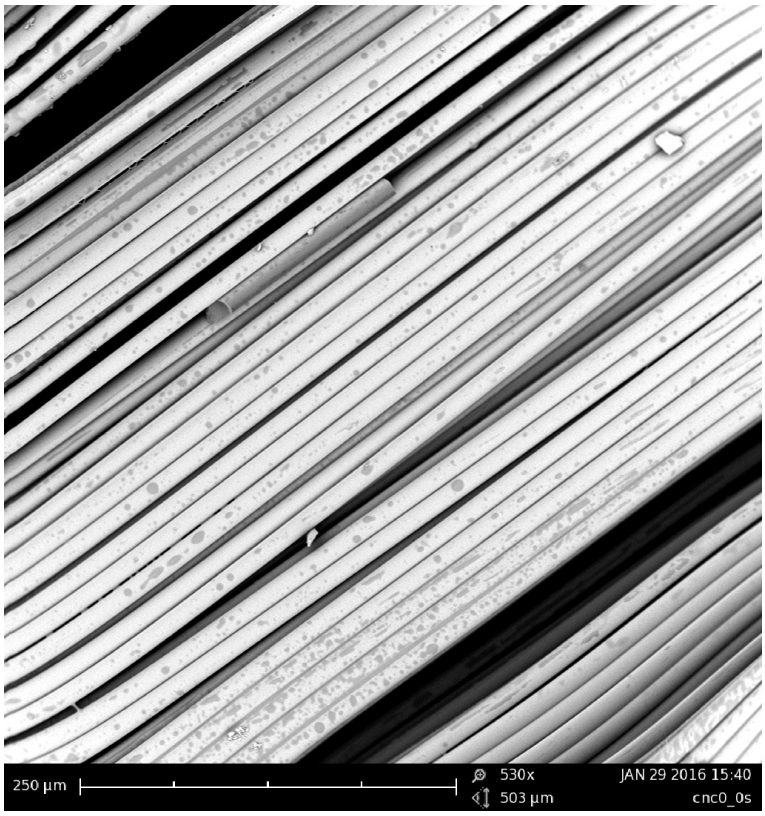

Figure 3.8: SEM Glass Fiber Coating (0s)

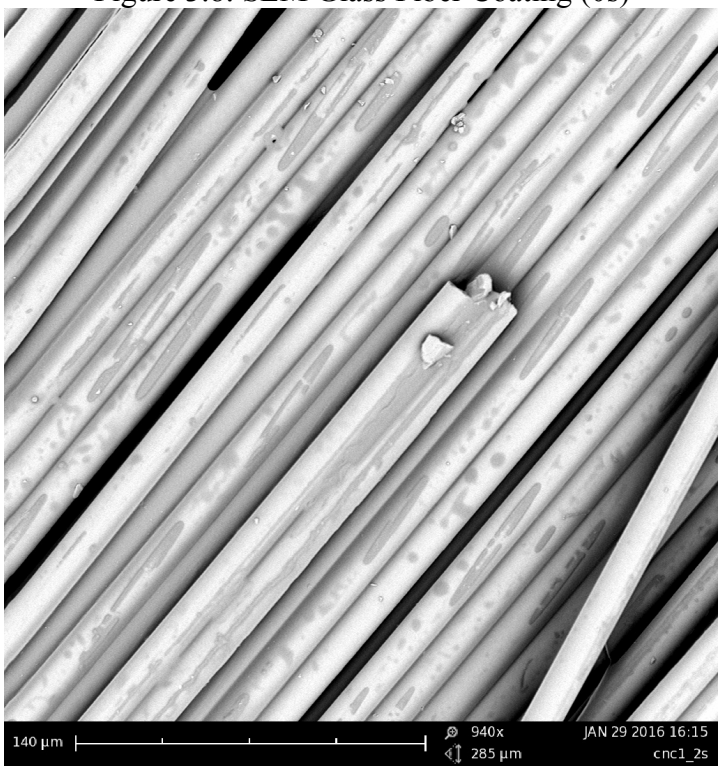

Figure 3.9: SEM Glass Fiber Coating (2s)

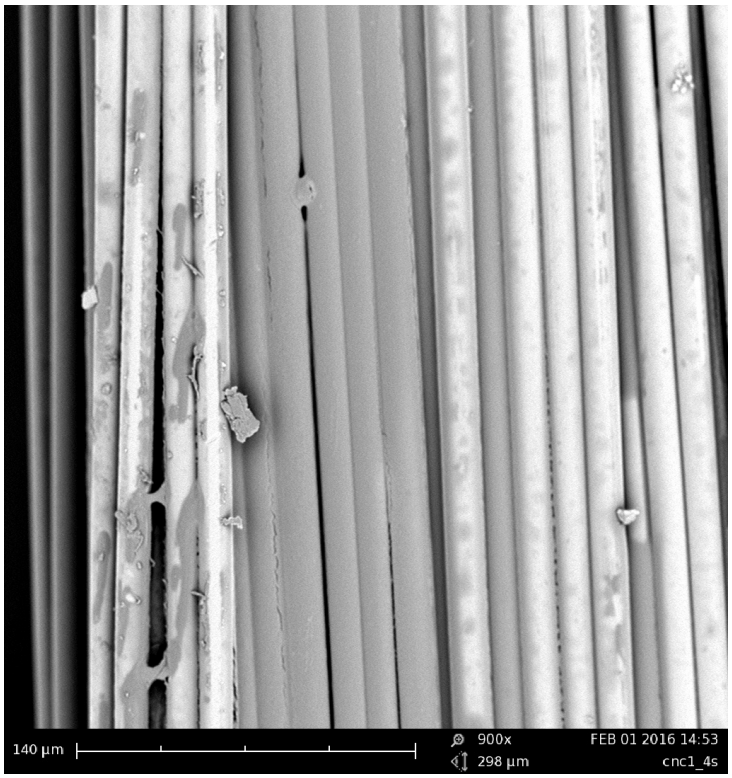

Figure 3.10: SEM Glass Fiber Coating (4s)

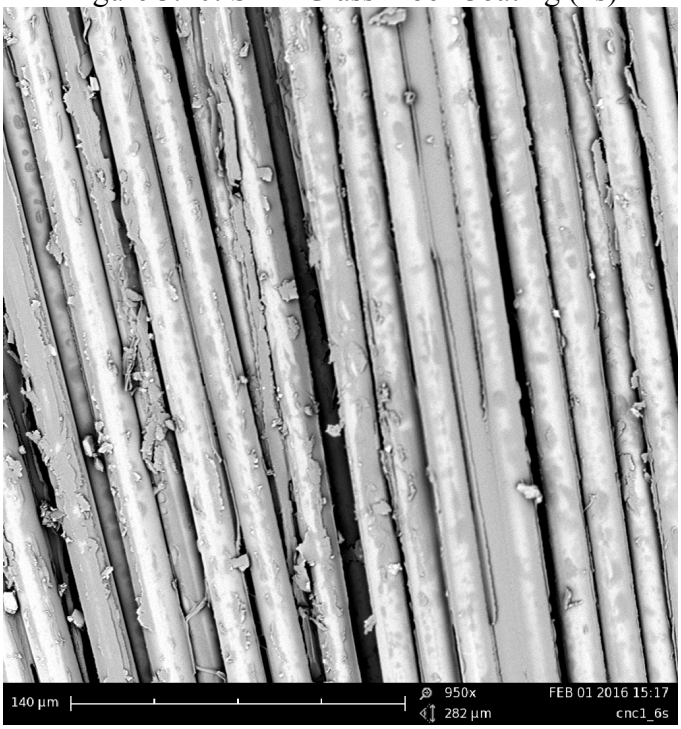

Figure 3.11: SEM Glass Fiber Coating (6s)

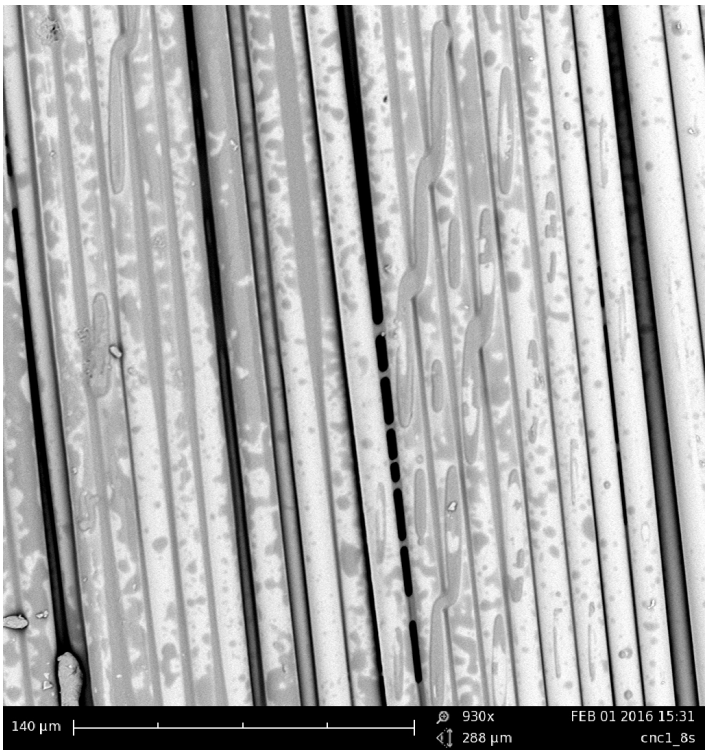

Figure 3.12: SEM Glass Fiber Coating (8s)

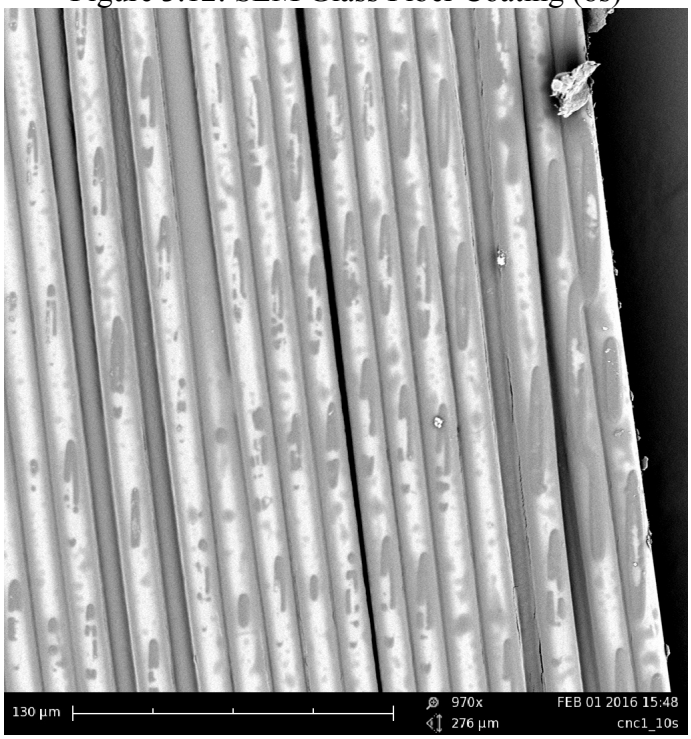

Figure 3.13: SEM Glass Fiber Coating (10s)

In Figure 3.14, the TGA results of the study quantitatively show the deposition of CNC for each immersion time. From this graph, it is clear that the optimal immersion time for maximum deposition is 6 seconds. It is interesting however, that even with minimal immersion time (i.e., 2s), there is clear CNC deposition on the glass fibers. Although there are large standard deviations for these results, this immersion time is used for the construction of the bath.

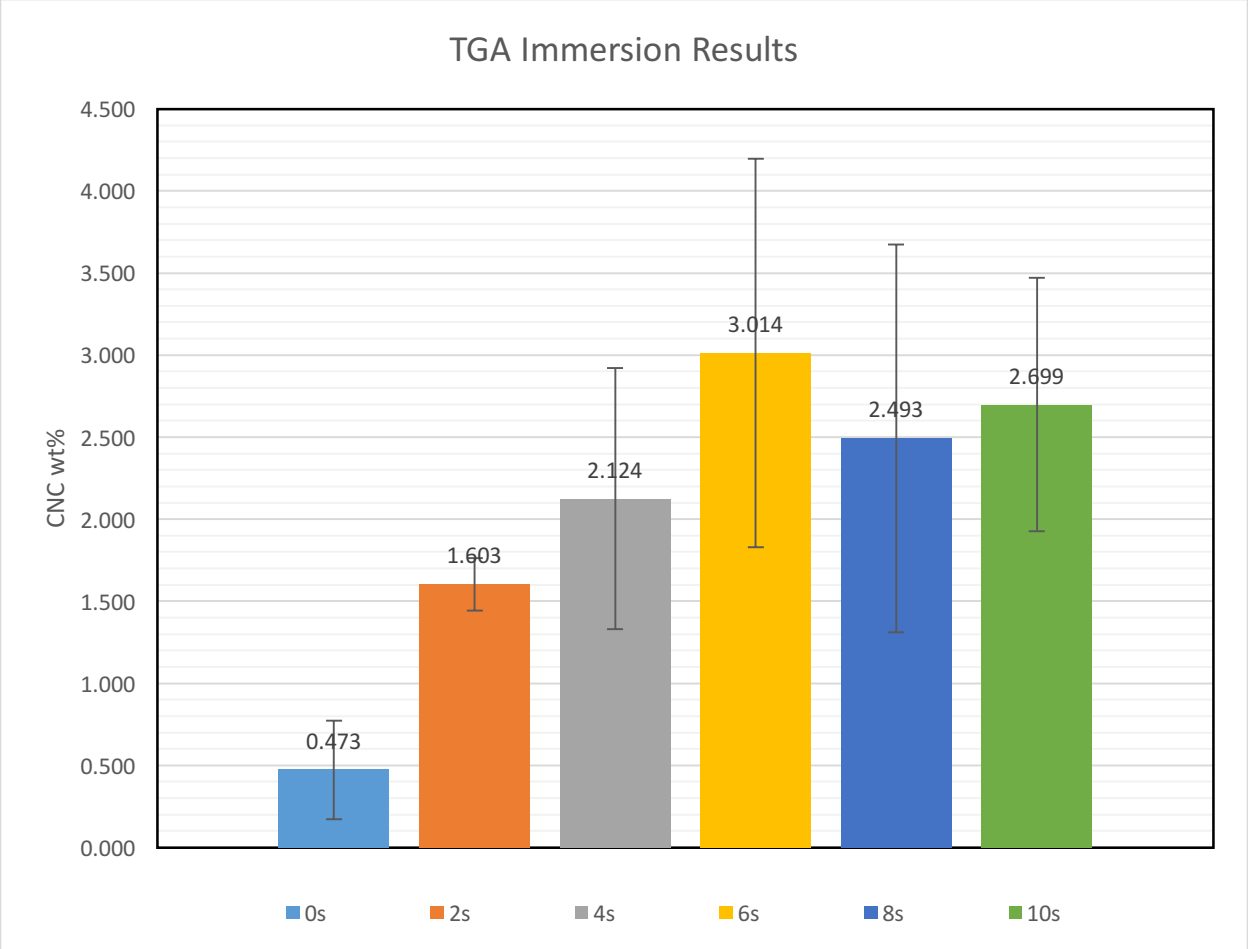

Figure 3.14: CNC Deposition as a Function of Immersion Time

3.3.2 Drying Time

Before the coated fibers are input into the SMC manufacturing line, the fibers need to be dried first such as to facilitate proper cutting and composite manufacturing.

The heat gun used to facilitate efficient drying is the Wagner HT1000 Heat Tool, which is capable of circulating hot air at 540ºC. To quantitatively measure how fast the heat gun will dry the glass fibers, one roving was immersed in a CNC bath for 6 seconds, then placed on a platform with the heat gun directly applied to the roving for a specific time until the roving was fully dried. Table 3.2 highlights the specific drying times for 10 rovings at the 540ºC heat setting. From this table, it can be shown that the average drying time for one roving given one heat gun is approximately 47.5 seconds, and is used for subsequent calculations for the dimensions of the CNC bath.

Table 3.2: List of Drying Times for 540ºC

Heating Times	
Trial	
1	1:03
2	47:85
3	46:36:00
4	51:85
5	44:50:00
6	49:42:00
7	1:37:00
8	49:13:00
9	43:72
10	51:93
AVG	**47:50:00**

3.3.3 Bath Design

Using the parameters determined in the previous two sections, the bath was constructed for the SMC settings as stated in Chapter 2. CNC deposition occurs at a minimum of two seconds, and the optimal drying time is 47.5 seconds, and given the SMC settings, a cut speed of 6.5 correlates with a fiber speed of 166 mm/s, thus requiring a bath length of 332 mm (13 in) and an effective drying length of 7,000 mm (275 in. or

23 x 12in passes). To be consistent with the drying results, four heat guns will be used for the four rovings passed into the SMC machine. To support the heat required for drying, the bath would need to be made entirely from aluminum so that it can be easily cut, welded, and machined. The final dimensions of the bath are shown is Figures 3.15 and 3.16.

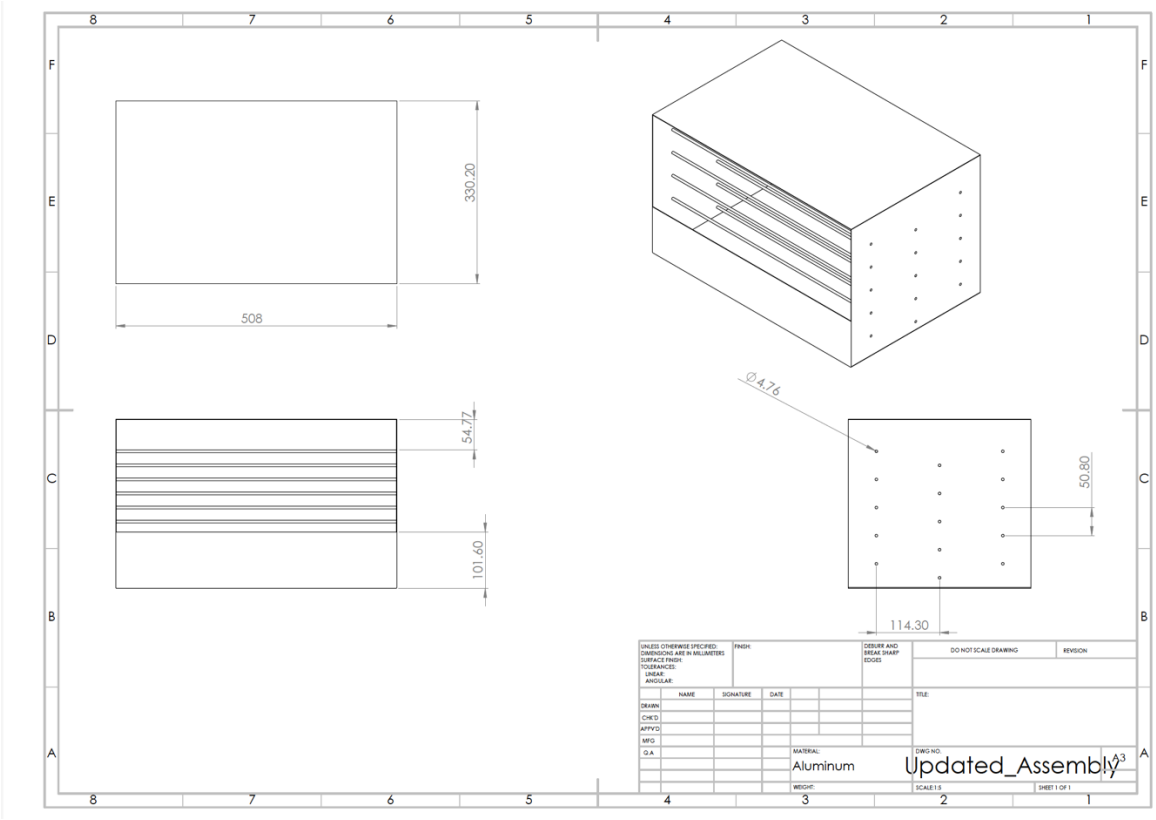

Figure 3.15: Engineering Drawing of Bath Design

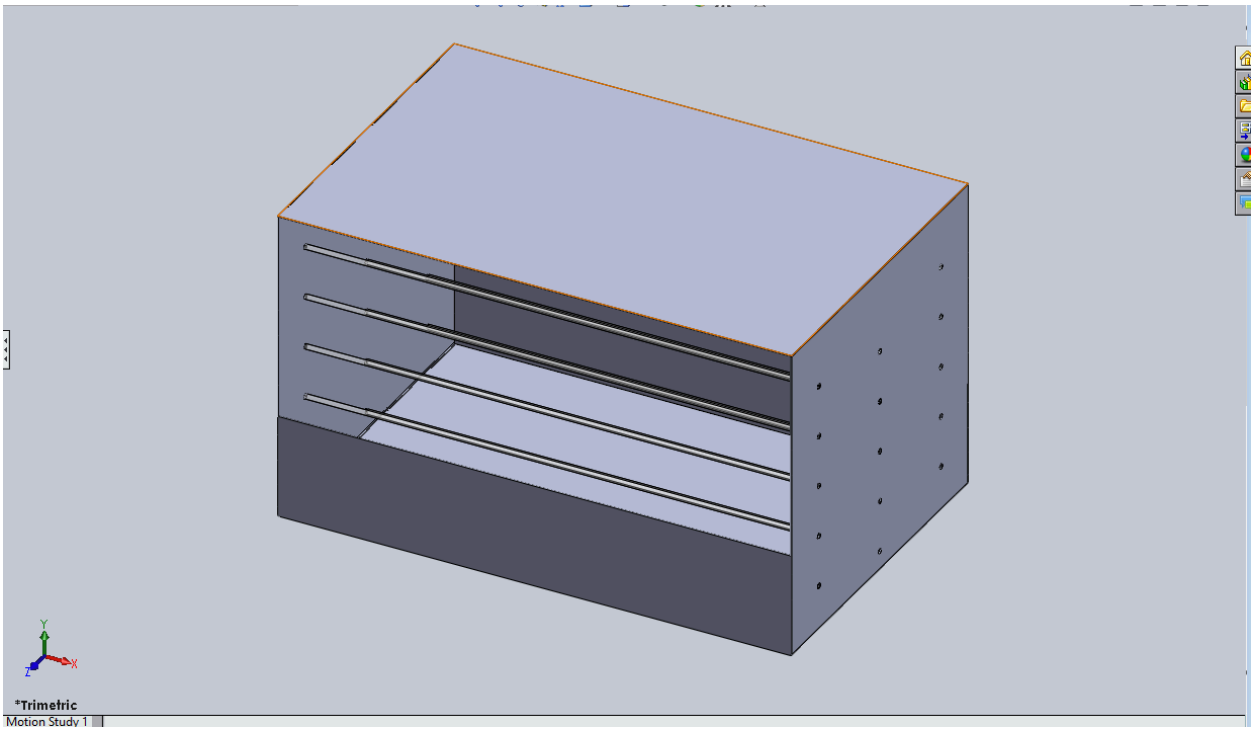

Figure 3.16: Isometric View of CNC Bath Design

3.3.4 Bath Construction and Integration

Given the based design of the CNC bath, some changes needed to be made such that the bath could be properly manufactured and implemented given the available resources. The bath and the necessary holes were cut from an aluminum sheet using a waterjet cutter, and then folded using a metal former to the appropriate angles to form a box-like structure. The ends were riveted and welded together to form the structure. The guiding rods were inserted into the holes and then cured epoxy held the rods in place such as to prevent lateral movement from running the glass fibers through them. However, fixing the rods in place does not allow the rods to rotate, and thus introduces friction to the GF as they are pulled through the bath. The bottom part of the bath was sealed to prevent water leaks to retain the CNC solution at the bottom of the bath, and the heat guns were placed within each of the two holes on each side. Finally, the bath was secured

to the fiber rack across from the SMC machine such that the fibers can be threaded through the bath, dried, and entered back into the SMC manufacturing line. Pictures of the coating set-up are shown in Figures 3.17-3.19. All of these steps were completed to allow for the successful coating, drying, and input of coated glass fibers into the manufacturing line.

While this design of the bath is functional, it can be improved in several aspects in order facilitate efficient coating and drying of the GF. Friction from the guiding rods can be addressed by incorporating high temperature polymeric rollers (i.e., Teflon) around the rods in the next bath design or by utilizing ball bearings with the current aluminum rods. To introduce fiber spreading of the entering GF rovings, an air knife can be used to separate and spread the glass fibers such that it would increase the surface area available for drying. Finally, to address fiber spreading of the exiting fibers, ceramic eyes can be used to both comb the fibers into their respective positions, and also scrape off excess moisture from the fibers prior to being input into the SMC machine.

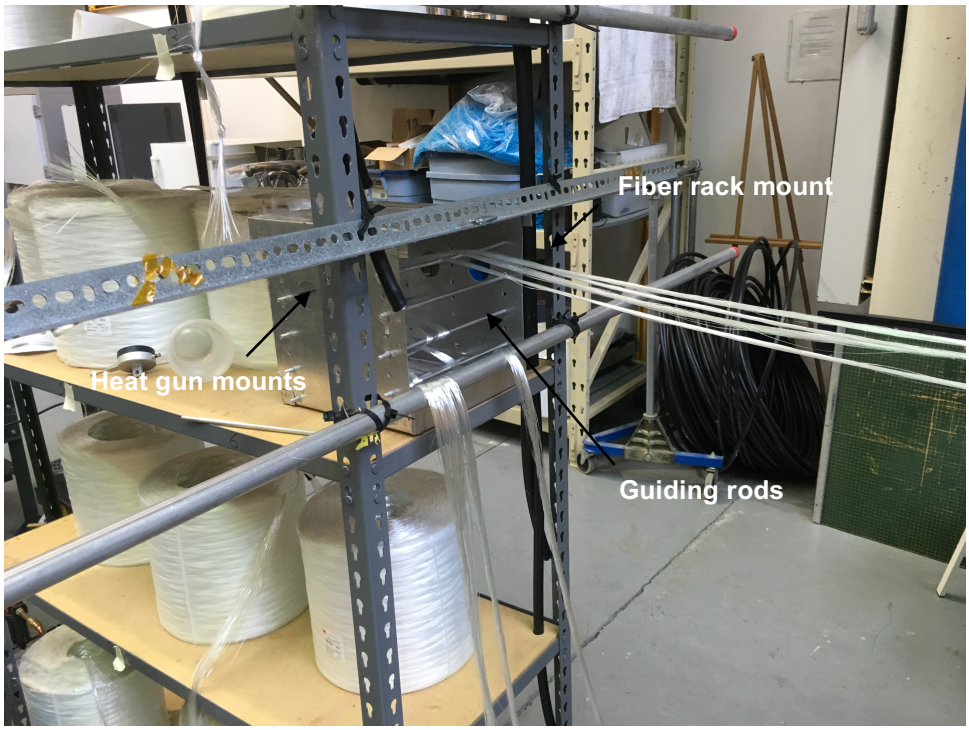

Figure 3.17: Set-up of CNC Bath

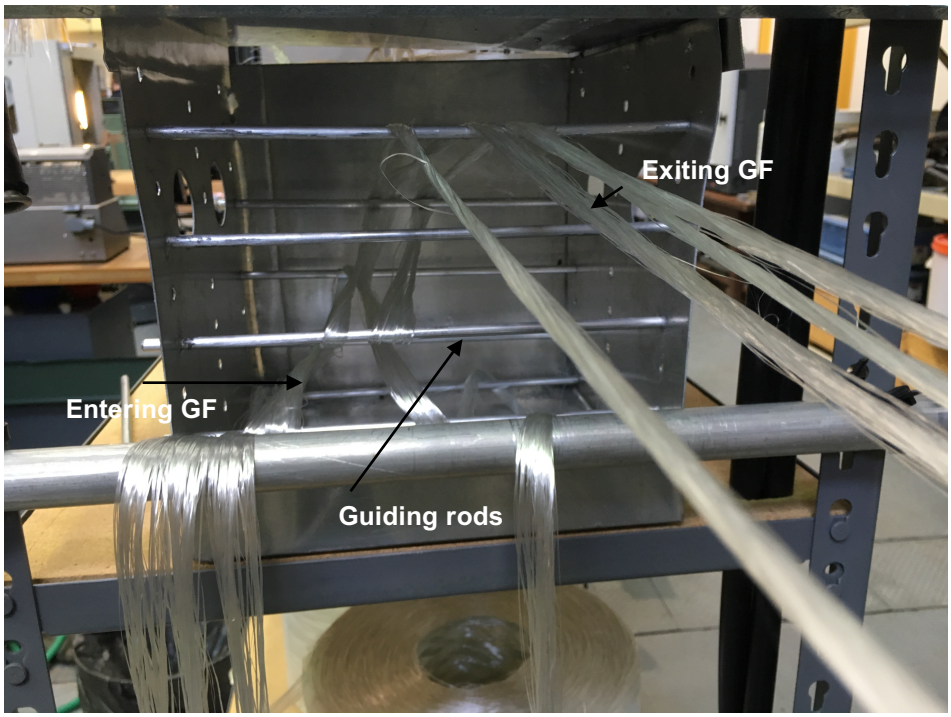

Figure 3.18: Glass Fibers passing through Guiding Rods

Figure 3.19: Glass fibers exiting and entering SMC line

3.4 Conclusions

This study demonstrated that introducing a small amount of CNC in the form of a coating on GF can enhance the IFSS and mechanical properties of short GF/epoxy composites without increasing the weight. The proposed mechanism for altering the composite properties is to improve the interfacial adhesion and stress transfer ability and rate across the GF/epoxy interface due to the CNC coating. Single fiber fragmentation tests showed that coating of GF up to 1.96 wt% CNC was able to increase IFSS. The CNC-GF/epoxy composites produced using CNC coated chopped GF roving showed increases in tensile and flexural properties, which were attributed to the increase in IFSS associated with the application of the GF coatings. The greatest improvement in properties occurred when 0.17 wt% CNC coating on GF rovings was used. Specifically,

the IFSS increased by 58%, the tensile elastic modulus and strength by ~10%, strain at break by ~14 %, the flexural modulus and strength by ~40% and flexural strain at break by ~9%. It is noted that the CNC coating did not significantly alter the rubbery modulus, T_g and tan δ. The results highlight that the use of CNC coatings on GF, is a possible approach for enhancing the mechanical properties of GF/epoxy composites with no weight penalty. Due to these newfound results, design and construction of a mechanism in which to coat and dry the fibers prior to entering the SMC manufacturing line was completed. This would allow for future projects which utilize the bath as a scalable method for coating the glass fibers prior to their use into the SMC line. The resulting composites would need to be characterized to verify that they are consistent with the lab-scale study presented in this chapter. This project would provide a mechanism for incorporation of CNC into industrial grade composites, and thus would improve the mechanical properties of the resulting composites. While this method was verified as a viable solution for incorporating CNC into SMC, another study to determine the validity of using CNC as an auxiliary reinforcement within the epoxy matrix to improve the mechanical properties was performed such as to offer yet another viable method for improving the mechanical properties of industrial grade composites by utilizing CNC.

CHAPTER 4

INCORPORATING CELLULOSE NANOCRYSTALS IN SHEET MOLDING COMPOUND (SMC)

While the coating of glass fibers using CNC has been confirmed as a valid mechanism for enhancing the mechanical properties of the resulting composites, utilizing CNC as an auxiliary reinforcement within the epoxy resin was suggested as an alternative mechanism for incorporating CNC with SMC composites. This chapter highlights the study performed to determine the effect CNC has on a composite produced in the SMC line by varying the amount of CNC within the epoxy resin. This study also determines the maximum amount of CNC that can be dispersed within the epoxy resin before agglomeration occurs. The main challenge behind this method is dispersion, which was mitigated through sonication of the CNC within the epoxy hardener.

4.1 Experimental Details

4.1.1 Materials

Manufacturing composites that are analogous to industrial grade composites requires a specific set of materials that are compatible with a sheet molding compound manufacturing line. Owens Corning (Oak Brook, IL, US) ME1510 multi end roving GF (TEX 4800, single filament diameter of 10 ±1 μm) were used in the SMC machine as received. The GF rovings were chopped in the SMC machine to an average length of 25±0.5 mm. A bicomponent epoxy resin consisting of 150 thick epoxy (diglycidyl ether of Bisphenol-A epoxy) and 556 slow amine hardener supplied by US Composites (Wes Palm Beach, FL) was used. Aerosil-Cabosil (fumed silica) supplied by US composites was also used as the thickening agent. CNC in the form of freeze-dried particles [39]

were supplied by the USDA Forest Service-Forest Products Laboratory (FPL), Madison, WI, USA. The average length and width of the CNC were 6.4 ± 0.6 and 138 ± 22 nm, respectively [40]. [40]. 3 mil thick, 15-inch wide polyethylene sheets were supplied by Plastic Suppliers Inc. as the release film for the final composites coming out of the SMC line. WD-40 was used as purchased as a release agent, as it was the most efficient for removing partially cured epoxy from the polyethylene sheets compared to other release agents. It is recognized that WD-40 is actually a solvent and may plasticize the resulting composites, and thus the obtained results for improving the mechanical properties may be higher than what has been obtained in this study, and is a point for further investigation.

4.1.2 Dispersing CNC in the resin

The resin used in the SMC production, consisting of CNC, hardener, monomer and thickening agent, was prepared in a two-step process: i) dispersion of the CNC in the hardener using sonication and ii) mixing the CNC-hardener suspension with the epoxy. The hardener was used as the dispersion medium for CNC due to its lower viscosity (~ 400 cP) compared to that of the epoxy (~ 19000 cP) leading to a more uniform CNC dispersion in the resin [35]. The desired amount of CNC (0-1.4 wt% in the resin) was stirred with 500 g hardener and then sonicated (UIP500hd heilscher ultrasonic processor, 34 mm probe diameter, amplitude of 90) for 8-20 min depending on CNC content, with longer times for higher contents. The sonication time was determined by visual inspection. A water bath was used during the sonication to keep the temperature at or less than 50 ˚C. Next, 60 g fumed silica thickening agent was mixed with the hardener-CNC suspension by manual stirring for 10 min at room temperature. Finally, 1000 g epoxy was added to the hardener-CNC-fumed silica mixture and manually stirred for 5 min. The

ratio of the epoxy to hardener was 2:1 wt% as proposed by the supplier. The prepared resin was used in the SMC line within ~10 min ensuring its viscosity remained in its abyss for the maximum wettability of the GF. The final concentration of the thickening agent in the resin was 4 wt%. Control resin with no CNC was prepared similarly. Resins with CNC concentrations of 0, 0.2, 0.4, 0.7 and 1.4 wt% were prepared using the above procedure.

4.1.3 Fabrication of SMC composites

GF/CNC-epoxy SMC composites were produced with a 35 wt% GF content. SMC materials of different CNC content were manufactured using a Finn and Fram SMC line at Georgia Tech. The basic difference between this SMC line and the larger scale industrial ones is the width of the SMC materials (0.3 m vs 0.9-1.5 m) indicating that the knowledge gained on the processing-structure-property of the resulting SMC composites can have industrial relevance.

In the SMC line, GF rovings, pulled through a set of cutters, were chopped to 25.4 mm long bundles, and thrown randomly on the lower resin layer and then covered with another, upper resin layer. The resin layers were supported and carried forward by a polyethylene carrier film. The resin amount was controlled by two doctor blade systems (upper and lower) and the reinforcing fiber length and content were controlled by the rotational speed of the cutters and speed of the conveyor belts respectively. Four GF rovings with a belt speed of 0.9 m/min were used in the production to achieve 35 wt% GF SMC composites. The glass fiber/resin sandwich structure passed through a set of compaction rollers, where entrapped air was removed and the fibers were fully impregnated and wetted by the resin. Each run of the SMC continued for 5-10 min, the

time the resin viscosity needs to reach its minimum value, to facilitate the fiber impregnation during compounding, but it remained sufficiently high to avoid resin leakage from the carrier film. Then, the process was manually stopped after the resin was completely consumed and the SMC was collected as a continuous sheet formed into a roll.

The length, width and thickness of the final SMC material made in each run were ~3 m, 254 mm, and 1.8 mm respectively. Next, the SMC roll was conditioned at room temperature for 2.5 h (set time proposed by the epoxy supplier) to allow the compound viscosity to reach a maturation state where the viscosity was sufficiently high to allow easy handling of the compound and sufficiently low to allow molding of the compound. For every CNC concentration, three 292×254×5.5 (and 3.5) mm^3 plaques were made, two plaques contained three SMC layers and one plaque contained two SMC layers, all of which were stacked on top of one another. SMC plaques with various thicknesses allowed investigation of the influence of thickness on mechanical properties. Then, the plaques were placed between two aluminum tool plates and hot pressed and cured at 124 kPa and 100 °C for 1 h, followed by post-curing at 120 °C for 2 h using a Carver 4122 manual heated press. The closing speed of the hot press was 7 cm/s (the maximum speed) for all of the batches. Maximum speed was required to minimize the effect of the SMC charge thickness on the resin flow pattern within the plaques. Since the plaques were made with only two or three layers (a thin charge), it is expected that the closing speed of the hot press would not significantly impact the resin flow pattern [45] and consequently the properties of the SMC composites. After the curing process was completed, the plaques remained at room temperature for 48 h prior to cutting and testing to prevent any

potential plastic deformation during handling/testing. The dimensions of the final plaques were 304×267×5 mm^3. The test coupons were cut from the plaques using a waterjet (MAXIEM 1515). The corresponding naming scheme for the GF/epoxy SMC composites is 35GF/*n*CNC-epoxy, where *n* is the CNC content in wt% in the composite. Table 4.1 shows the equivalent CNC concentration in the hardener, resin (CNC + hardener + epoxy + thickening agent) and 35GF/*n*CNC-epoxy SMC composites. In addition, test coupons from the neat epoxy (no CNC) and 1.4CNC-epoxy composite (the highest CNC concentration as shown in Table 4.1) were made by pouring the prepared resin in a mold followed by the same curing process. No thickening agent was used in making these samples to better understand the effect of CNC on the mechanical properties of the CNC reinforced epoxy.

Table 4.1: Equivalent CNC content in hardener, resin and 35GF/*n*CNC-epoxy SMC composites

Material	CNC content (wt%)				
Hardener 556	0	0.6	1.2	2.1	4.3
Resin	0	0.2	0.4	0.7	1.4
Composite	0	0.15	0.3	0.5	0.9
	GF content (wt%)				
	35±6		35±6		

4.1.4 Characterization techniques

A Phenom G2 Pro (Phenom-World BV) scanning electron microscope (SEM) at an acceleration of 5 kV was used to study the fracture surface of the SMC composites. A plasma sputter (Ted Pella Inc.) was used to apply gold coating on the surface of the samples prior to SEM imaging to minimize charging.

Water displacement method was used to measure the specific density of the SMC composites according to ASTM D-792. Thermo-gravimetric analysis (TGA), using TGA

SDT Q600 (TA Instruments), was used to determine the GF content in the composites. The samples were heated from 50 °C to 500 °C at 10 °C/min in inert atmosphere. Each TGA data point is an average of at least 12 measurements.

The tensile properties of the CNC-epoxy and SMC composites were determined according to ASTM D638 using an Instron 33R 4466 equipped with 10 kN load cell for dog bone samples with a gauge length of 57 mm, width of 13.1mm and thickness of 5mm. An extensometer, Instron 2630-106, with a gauge length of 25 mm was used to record the axial strain. The modulus was calculated between the axial strain values of 0.05% and 0.2%. The flexural properties were measured using three-point bending tests with an Instron 33R 4466 equipped with 10 kN load cell according to ASTM D790-02 with a support span of 50 mm and thickness of 5 mm at a displacement rate of 2.15 mm/min. Each tensile and flexural data point is an average of at least eight tests.

The impact energy was measured using Charpy with no notch tests with an Instron SI series pendulum impact tester with a maximum impact head of 406.7 J (300 ft-lbf) according to ISO179 with a support span of 43 mm for 12.7 mm wide and ~5 mm thick rectangular samples. Each data point is an average of at least seven tests.

Dynamic mechanical thermal analyses (DMA Q800, TA Instruments) in three-point bending mode with a support span of 50 mm was used to measure the storage and rubbery moduli and the glass transition temperature (T_g) in the 25 °C −160 °C range at a heating rate of 5 °C /min and 1 Hz. A preload of 0.01 N and a maximum strain of 0.05% were applied on rectangular 12.7 mm and ~5 mm thick specimens. Each data point is an average of at least three tests.

4.2 Results and discussion

4.2.1 Specific density, CNC content and thermal stability

The density for all the SMC composites was found to be 1.6 ± 0.03 g/cm^3 independent of the CNC content, which was expected considering the small CNC wt% used. The GF wt% for SMC composites with CNC content of 0 and 0.3 is shown in Table 2. GF content was measured using samples from different locations of the composite plaque. Although the SMC composites were designed to contain 35 wt% GF in the SMC line, a deviation of ±6 wt% indicates that more fibers were thrown at the center of the SMC material compared to the edges resulting in higher GF content at central locations.

4.2.2 Fracture surface morphology

The morphology of the fracture surfaces of the SMC composites failed in the tensile testing was studied using a SEM. In general, CNC addition appeared to have altered both the matrix phase properties and the GF/matrix interfacial interactions both of which can contribute to higher mechanical properties of the GF/CNC-epoxy SMC composites. Compared to the smooth fracture surface of the SMC composites with no CNC shown in Figure 4.1 (a) − (c), adding CNC in the epoxy matrix resulted in a rougher fracture surface as shown in Figure 4.1 (d) and (e), suggesting CNC addition has altered the matrix properties. Furthermore, the main failure mechanism for GF/epoxy SMC composites without CNC was interfacial debonding as indicated by the clean fiber pull-outs devoid of the matrix shown in Figure 4.1 (c) and smooth cavity traces created by the pulled out fibers shown in Figure 4.1 (a), suggesting weak fiber-matrix adhesion. In contrast, by adding CNC in the epoxy, although the main failure mechanism still remained the fiber pull-out, concurrent matrix cracking, fiber breakage and interfacial debonding, as can be seen in Figure 4.1 (d) and 4.1 (f) were also observed as a result of

matrix strengthening by CNC. These mechanisms lead to an increase in the absorbed energy in fracture. Also, matrix residues on the pulled-out fibers, shown in Figure 4.1 (f), appeared to increase with increase in the CNC content (not shown in the images), compared to the clean pulled out fibers in the SMC composites with no CNC, shown in Figure 4.1 (c), indicating an improvement in the GF-matrix adhesion.

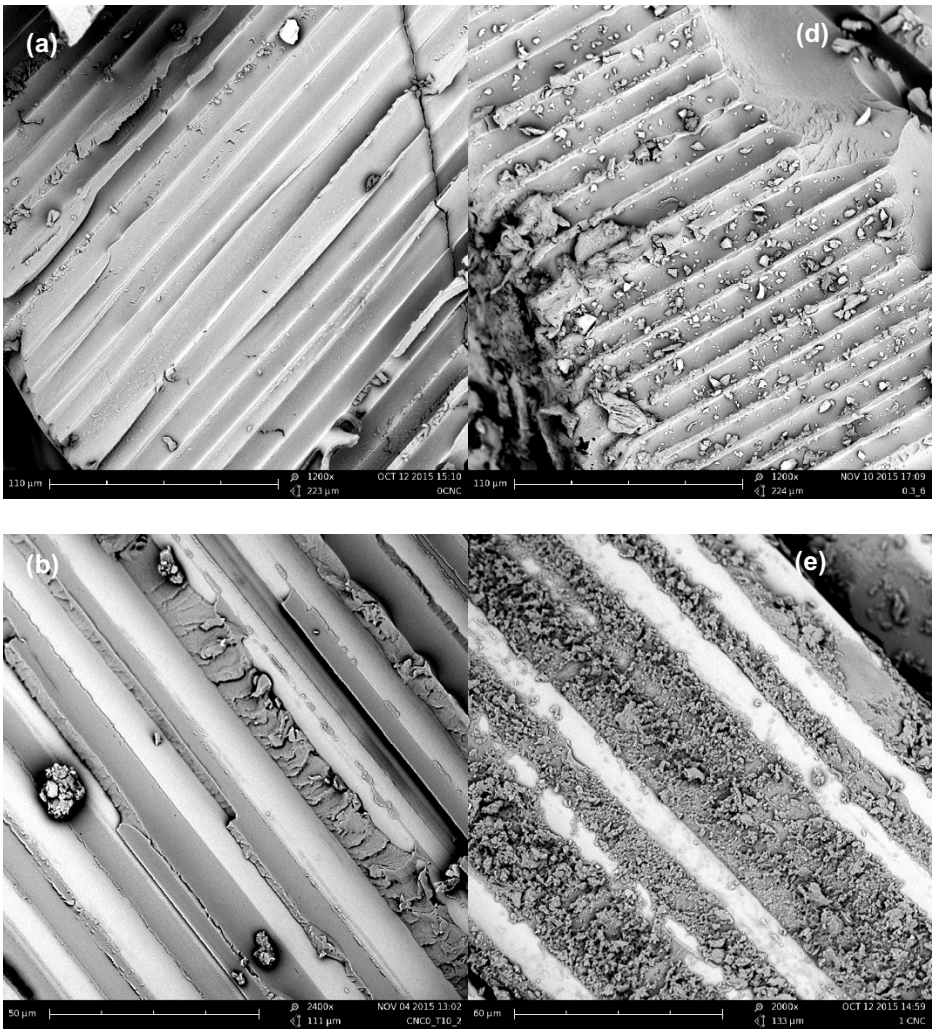

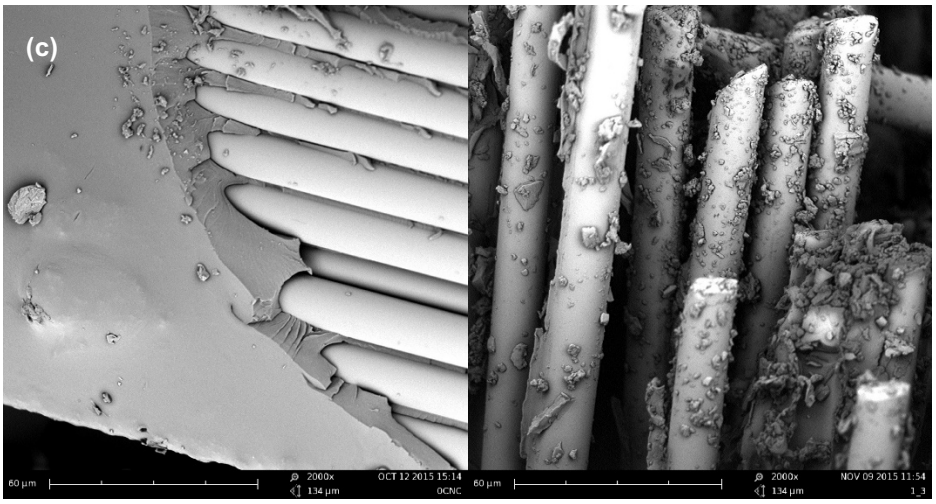

Figure 4.1: SEM images for tensile fracture surface of different composites(a) – (c) 35GF/epoxy, (d) and (e) 35GF/0.15CNC-epoxy (f) 35GF/0.9CNC-epoxy

4.2.3 Thermomechanical properties

The thermomechanical properties of the CNC-epoxy (0 and 1.4 wt% CNC) and SMC composites below and above T_g are presented in Table 4. At 25 °C (below T_g), addition of 1.4 wt% CNC enhanced both the storage (E') and rubbery modulus (E_r: the storage modulus above T_g at T=115 ^{o}C) by 34% and 77% respectively, demonstrating the reinforcing effect of CNC. The CNC did not impact the T_g and tan δ.

In SMC composites with lower CNC content, there was minimal influence on the storage modulus, but for 0.5 wt% and 0.9 wt% of CNC the E' of the corresponding SMC composites slightly increased by ~9% as compared to that of 35GF/epoxy composites as summarized in Table 4.2. The increase in the storage modulus at 25°C can be attributed to the CNC stiffening effect. In contrast, at 115°C (above T_g), the addition of CNC in the epoxy matrix, significantly enhanced the rubbery moduli of the SMC composites by ~30-40% for CNC content of 0.3, 0.5 and 0.9 wt%. Such an increase has been attributed to the formation of a percolated CNC network [31, 33, 49], but this may not be the case in this

study as the volume fraction of CNC in the epoxy is low (up to 1.4%, Table 4.1). However, an increase in the rubbery modulus may imply that CNC inhibited the chain segmental motion in the epoxy polymer above T_g, which is directly related to the rubbery modulus. The presence of CNC in the composite up to 0.9 wt% has no effect on the tan δ and the T_g of the corresponding composites. Moreover, it was found that the thickness (3.5- 5.5 mm in this study) of the SMC composites did not influence the viscoelastic properties.

Table 4.2: Viscoelastic properties of *m*CNC-epoxy (*m* is CNC wt% in epoxy) and 35GF/*n*CNC-epoxy SMC composites (*n* is CNC wt% in epoxy) in three-point bending mode

Composite	E' @ 25 °C (GPa)	E_r @ 115 °C (MPa)	T_g (°C)	tan δ @ T_g
Epoxy	2.01±0.14	5.7±0.8	81.6±1.1	0.89±0.02
1.4CNC-Epoxy	2.75±0.19	10.1±0.9	82.5±1.4	0.94±0.04
35GF/epoxy	6.46±0.15	200±13	73.8±0.2	0.53±0.01
35GF/0.15CNC-epoxy	6.54±0.09	194±7	72.1±0.3	0.48±0.01
35GF/0.3CNC-epoxy	6.3±0.11	295±20	72.8±0.3	0.51±0.01
35GF/0.5CNC-epoxy	6.90±0.10	264±27	71.2±0.6	0.53±0.01
35GF/0.9CNC-epoxy	6.859±0.08	292±38	72.3±0.7	0.51±0.02

E': storage modulus
E_r: rubbery modulus
T_g: glass transition temperature measured at in tan δ peak
tan δ: value of tan δ peak
Note: Error bars are 1 standard deviation.

4.2.4 Mechanical properties

The effect of the CNC content in the epoxy and SMC composites on the tensile and flexural properties of 35GF/CNC-epoxy composites is plotted in Figures 4.2 and 4.3. The incorporation of 1.4 wt% CNC in the epoxy matrix increased the elastic modulus of the CNC-epoxy composites by ~25% compared to the epoxy with no CNC as shown in Figure 4.2, demonstrating the reinforcing effect of the CNC. The elastic modulus of the equivalent SMC composites with CNC content of 0.9 wt% increased by 25% compared

to the control SMC composite i.e., 35GF/epoxy, which is identical to the modulus enhancement of the 1.4CNC-epoxy composite. For SMC composites with 0.15 wt%, 0.3 wt%, and 0.5 wt% CNC, the changes in elastic modulus of the corresponding SMC composites were not statistically significant. The modulus enhancement for SMC composites with 0.9 wt% CNC is believed to be due to stiffening of the matrix as a result of increase in the apparent modulus of the epoxy due to addition of CNC, as the CNC modulus (~100-220 GPa) is much higher than that of the epoxy (~ 3 GPa).

Also, the modulus enhancement in SMC composites may be due to increase in the apparent modulus of the GF/epoxy interphase as reported also in [45]. A stiffer interface results in faster stress transfer across the fiber/matrix interface and thus in higher modulus for the composite [46]. Gao et al. [47] reported that increase in the apparent modulus of GF/epoxy interface resulted in increase in the composite macroscopic modulus. In a recent study by the authors [50], incorporation of 0.17 wt% CNC as a coating to GF modified the GF/CNC/epoxy interphase and resulted in increases in the tensile and flexural moduli by ~10% and 40%, respectively. In the current study, the fracture morphology results discussed, as well as the increase in the modulus of composites with CNC, suggest that the CNC addition may have increased the apparent modulus of the GF/CNC-epoxy interface. However, it is difficult to ascertain the relative contribution of this mechanism in the modulus enhancement without relevant experimental results (e.g., atomic force microscopy).

The tensile strength of the GF/CNC-epoxy SMC composites increased by 30% for SMC composites with 0.9 wt% of CNC. For addition of 0.15 wt%, 0.3 wt% and 0.5 wt% CNC, the changes in tensile strength of the corresponding SMC composites are not

statistically relevant. The increase in the tensile strength in 35GF/0.9CNC-epoxy SMC composites is believed to result from stronger fiber-matrix adhesion and hence, a higher interfacial shear strength due to presence of CNC, as discussed in Section 3.2.2, inferring better stress transfer across the GF/CNC-epoxy interface as reported elsewhere [48].

Addition of CNC in the epoxy reduced the elongation at break by ~45% for CNC-epoxy composites compared to neat epoxy samples, as shown in Figure 4.2. The average value of the elongation at break for composites with 0.9 wt% was higher by ~ 22% compared to that of SMC composites with no CNC. Furthermore, the tensile work of fracture (the area under stress-strain curve), reported in Figure 4.3, indicates an increase by ~49% for SMC composites containing 0.9 wt% CNC, respectively as compared to that of SMC composites with no CNC, suggesting higher energy absorption before the catastrophic failure.

The flexural properties, summarized in Figures 4.2 and 4.3, show similar trends to those observed for the tensile properties. With addition of 1.4 wt% CNC in the epoxy, the flexural modulus of CNC-epoxy increased 57% while no statistically significant change in the flexural strength was recorded. No significant change in the flexural modulus and strength was observed for SMC composites with 0.15 wt%, 0.3 wt% and 0.5 wt% CNC. Large enhancements ~ of 44% and ~ 33% were recorded for the flexural modulus and strength respectively in SMC composites containing 0.9 wt% of CNC, as depicted in Figure 4.3. The enhancements are reported with respect to SMC composites with no CNC. There was no effect of the CNC content on the strain at break. Moreover, no change was observed on the impact energy of GF/CNC-epoxy SMC composites, shown in Figure 4.4, inferring that addition of CNC does not alter the impact energy of

SMC composites. It was also observed that the thickness of the SMC composite (3.5 and 5.5 mm) did not influence the mechanical properties.

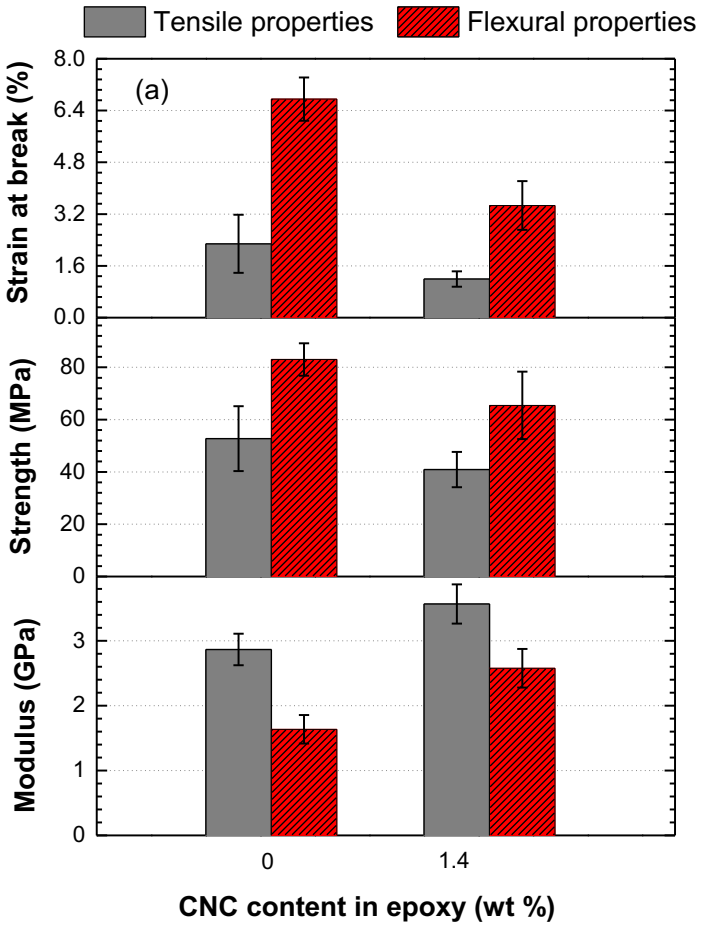

Figure 4.2: Effect of the CNC content in CNC-epoxy composites on tensile and flexural properties. Error bars are 1 standard deviation.

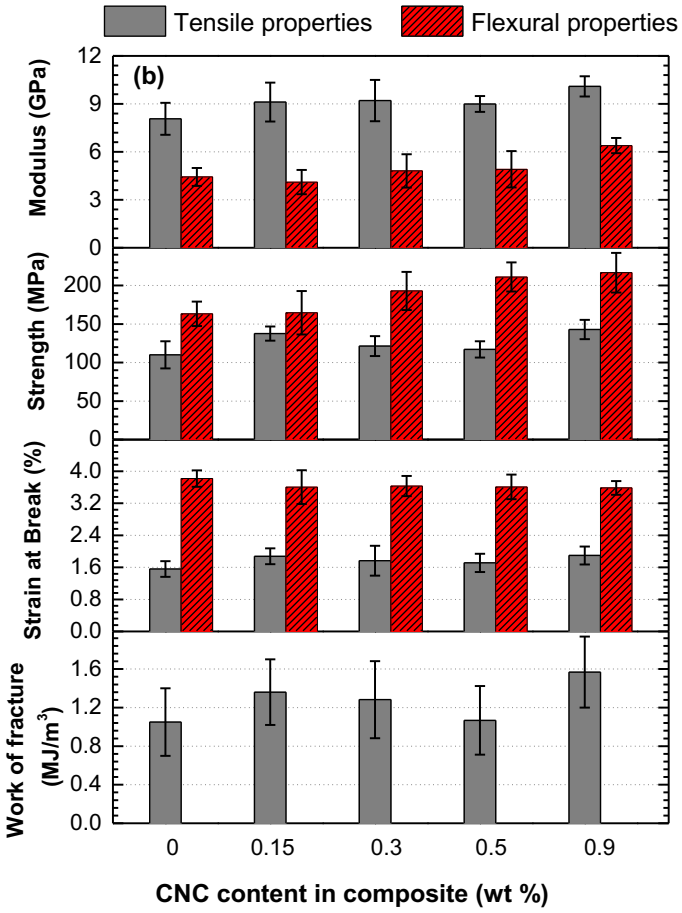

Figure 4.3: Effect of the CNC content in 35GF/CNC-epoxy SMC composites on tensile and flexural properties. Error bars are 1 standard deviation.

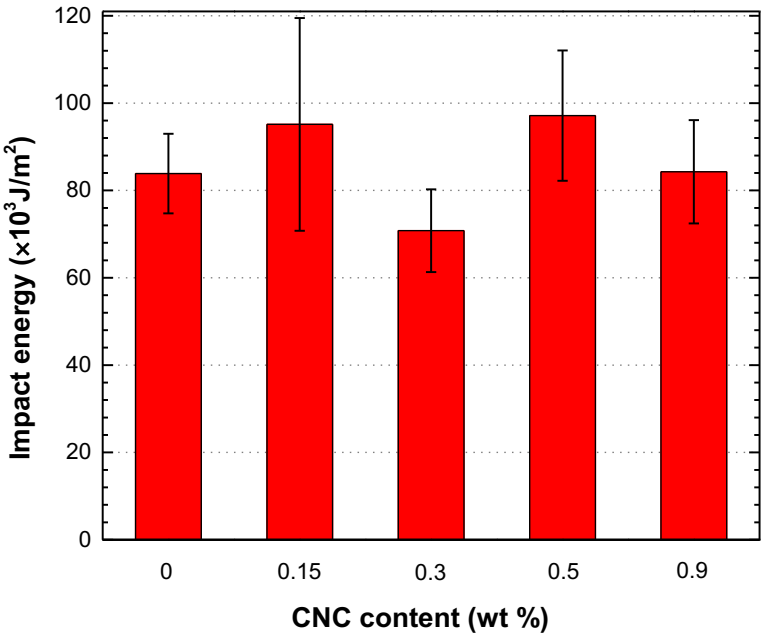

Figure 4.4: Effect of the CNC content (wt% in the composite) in 35GF/CNC-epoxy SMC composites on impact energy. Error bars are 1 standard deviation.

Overall, the addition of CNC resulted in improvements of the tensile and flexural properties of the corresponding SMC composites without any effect on the impact properties. However, the standard deviation for some results was high. One possible reason maybe the CNC agglomeration within the epoxy resin causes phase separation or void formation. CNC agglomeration or non-uniform dispersion in the epoxy can result in fluctuation in the strength values, whereas void formation in the epoxy or around the GF would lower the stress transfer efficiency and create stress concentration points resulting in premature failure.

It is also noted that the above uncertainty can be a result of the SMC manufacturing process. Specifically, there is inherent variability of the GF content within the SMC composites i.e., fiber rich or resin rich areas, a result of the pressure either

during the compaction and/or the compression molding process that results in resin flowing outwards. In order to investigate this phenomenon, 15 tensile coupons were cut from a SMC composite plaque containing 0.3 wt% of CNC. The location of each coupon within the plaque and with respect to the SMC line direction was recorded and is shown in Figure 4.5. The results of the tensile testing presented in Table 4.3 indicate that the tensile modulus and strength of the coupons located at the sides of the plaque with respect to the SMC production direction, i.e., coupons 1, 2 and 15 (Figure 4.5), were lower compared to the corresponding properties of the coupons located in the center. It appears that the edges of the SMC materials were richer in resin compared to the center due to spreading the resin toward the sides when passing through the compaction zone. According to the TGA results (see Section 3.2.3), central locations of the SMC materials contained more fibers compared to the edges resulting in higher GF concentration at the central locations of the SMC composite plaque.

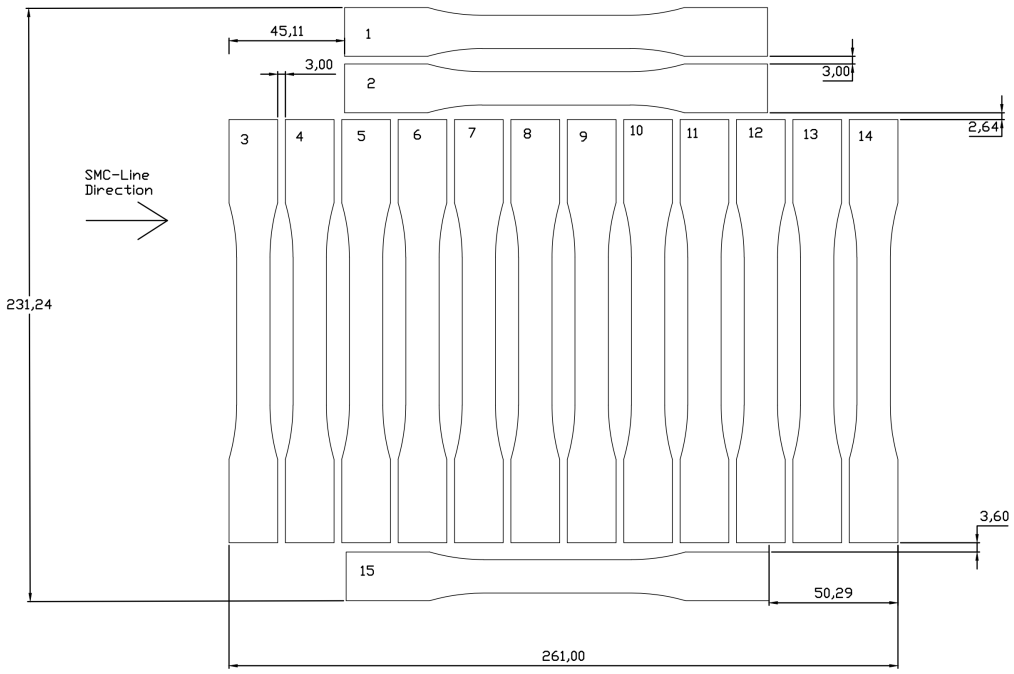

Figure 4.5: Tensile coupon locations cut from 35GF/0.3CNC-epoxy SMC plaque

Table 4.3: Tensile mechanical properties of 35GF/0.3CNC-epoxy SMC composite with respect to the location of the coupons

Sample	Strength (MPa)	Modulus (GPa)	Elongation at break (%)
1	53.23	7.57	0.50
2	59.81	6.05	1.13
3	91.61	8.08	1.32
4	90.61	8.21	1.23
5	98.75	7.43	1.53
6	94.22	6.79	1.39
7	93.60	6.19	1.55
8	98.40	7.77	1.35
9	98.98	14.41	1.22
10	112.54	8.63	2.04
11	88.74	9.66	1.39
12	88.58	11.95	0.85
13	121.30	9.74	1.42
14	106.31	10.73	0.97
15	77.44	6.92	1.31
Average	91.61	8.68	1.28
1 Standard deviation	17.13	2.23	0.33

4.2.5 Micromechanical model comparison

Table 4.4 compares the properties for SMC composite containing 0 wt% and 0.9 wt% CNC with those predicted by a micromechanical model developed for short fiber reinforced composites [51] as given in Eq. (1).

$$E_{Composite} = \frac{3}{8}E_{11} + \frac{5}{8}E_{22} \tag{1}$$

in which,

$$E_{11} = E_m\left(1 + 2\frac{l_f}{d_f}\eta_L v_f\right)/\left(1 - \eta_L v_f\right)$$
$$E_{22} = E_m\left(1 + 2\eta_L v_f\right)/\left(1 - \eta_L v_f\right) \tag{2}$$

$$\eta_L = \left(\frac{E_f}{E_m} - 1\right) / \left(\frac{E_f}{E_m} + 2\frac{l_f}{d_f}\right)$$
$$\eta_T = \left(\frac{E_f}{E_m} - 1\right) / \left(\frac{E_f}{E_m} + 2\right) \quad (3)$$

where l_f is fiber length, d_f is fiber diameter, v_f is fiber volume fraction, and E_f and E_m are the fiber and resin moduli. v_f and ρ_c (composite density) are calculated using Eq. (4) and (5).

$$v_f = \frac{w_f / \rho_f}{(w_f / \rho_f) + (w_m / \rho_m)} \quad (4)$$

$$\rho_c = \frac{1}{(w_f / \rho_f) + (w_m / \rho_m)} \quad (5)$$

where w_f and w_m are mass fraction, and ρ_f and ρ_m are density of the fiber and matrix respectively.

The properties of the epoxy and GF are also shown in Table 4.5. The elastic modulus of the epoxy and 1.4CNC-epoxy, obtained experimentally, are shown in Figure 4.2. The apparent modulus of the epoxy matrix in SMC composites with 0.9 wt% CNC is the mean value of the experimental elastic modulus of the 1.4CNC-epoxy composite, i.e. 3.6 GPa. The experimental results for elastic modulus and density for SMC composites with and without CNC are in good agreement with the predicted results, as summarized in Table 4.5 delineating the reinforcing effect of CNC in SMC composites.

Table 4.4: Properties of the GF and CNC-epoxy

Material	ρ (g/cm^3)	E GPa)	w (%)	v_{GF} (%)
GF	2.5	70	35±3	22±2
Epoxy	1.3	2.8± 0.2	65±3	78±2
1.4CNC-epoxy	1.3	3.6± 0.3	65±3	78±2

Table 4.5: Predicted vs. experimental modulus and density for 35GF/CNC-epoxy SMC composites

Sample	$E_{c,\ model}$ (GPa)	$E_{c,\ Exp}$ (GPa)	$\rho_{c,\ model}$ (g/cm^3)	$\rho_{c,\ Exp}$ (g/cm^3)
35GF/epoxy	8.0	8.1± 0.9	1.6	1.6± 0.03
35GF/0.9CNC-epoxy	9.3	10.1± 0.7	1.6	1.6± 0.03

l_{GF}/d_{GF}= 25
$E_{c,\ model}$: Predicted composite elastic modulus
$E_{c,\ exp}$: Experimental composite elastic modulus

4.3 Conclusions

In this study, CNC were added as reinforcements in epoxy resin used in the SMC manufacturing process. It was demonstrated that a small amount of CNC can enhance the mechanical properties of short GF/CNC-epoxy SMC composites without increasing the weight. The proposed mechanisms for altering the SMC composite properties with CNC additions were the enhancement of the effective properties of the epoxy matrix, improvement the interfacial adhesion, and stress transfer ability across the GF/matrix interphase. Improvements in tensile and flexural properties occurred by incorporation of CNC in the 35GF/epoxy SMC composites; specifically, introducing 0.9 wt% CNC resulted in increases in tensile modulus by 25%, tensile strength by 30%, tensile strain at break by 22%, work of fracture by 49%, flexural modulus by 44% and flexural strength by 33%. Also, it was found that introducing CNC up to 0.9 wt% in the SMC composites did not alter the impact energy. Moreover, the predictions for modulus and density using a micromechanical model for short fiber reinforced composites compared well with the obtained experimental results. These results highlight the potential of CNC for enhancing the mechanical properties of short GF/epoxy SMC composites with no weight penalty

using SMC production method, and thus a potential path toward high volume automotive composite production.

CHAPTER 5

CONCLUSIONS AND FUTURE WORK

The studies presented in this thesis have shown that the addition of CNC to polymer matrix composites can increase the macro-mechanical properties of the overall composite by contributing to individual components on a nano-scale. The two methods explored in this study which CNC may be incorporated into SMC includes as a coating, in which the interfacial properties between the glass fibers and the epoxy matrix is enhanced, and as an auxiliary reinforcement in the epoxy, in which the CNC facilitates load transfer more efficiently from the epoxy matrix to the glass fibers. Each of these methods provide a solution for increasing the macro-mechanical properties of the overall composite without compromising the density of the overall composite. This can allow for a reduction in weight by removing a portion of the heavier components (i.e. glass fibers) and replacing them with lighter components (i.e. CNC) to retain the mechanical properties, thus achieving the 6-8% increase in fuel efficiency associated with a 10% decrease in weight [1]. In addition, the studies have also highlighted a process in which CNC may be incorporated into SMC at a scalable level for industrial purposes, as may be used in the automotive and water vehicle industries.

5.1 CNC Coating of Glass Fibers for SMC

As highlighted in Chapter 3, the interfacial shear strength (IFSS) between the glass fibers and the epoxy matrix was increased as a result of the addition of CNC by means of coating and drying of the fiber. The IFSS results were found by means of a single-fiber fragmentation test, in which the average length of the fiber fractures was used to determine the IFSS. It was shown that the IFSS will increase up to 1.96 wt% CNC in

water, and then the IFSS will decrease due to agglomeration. The increase in IFSS may be attributed to increased surface roughness and adhesion between the glass fibers and the epoxy. The optimal IFSS was achieved by coating the glass fibers with a 1% CNC wt% solution in water, which corresponds to 0.17 wt% within the composite, in which the IFSS will increase by 58% as compared to uncoated fibers. Due to this increase in the IFSS, the resulting composite showed a 10% increase in tensile strength and a 40% increase in flexural strength. Design and construction of a coating bath was completed and provides an autonomous, scalable mechanism in which glass fibers may be coated and input into the SMC manufacturing line.

5.2 CNC-Epoxy Reinforcement for SMC

CNC was able to be incorporated easiest into the SMC manufacturing line by dispersing the CNC into the epoxy resin before being input into the line. The results from the study in Chapter 4 show that this method is a scalable and valid method for improving the macro-mechanical properties of the resulting composites. Dispersion of the CNC into the epoxy was best facilitated via sonication within the hardener, which had the lowest viscosity. The monomer was then added to the epoxy and used within the SMC line. The addition of the CNC did not alter the viscosity or the curing behavior of the epoxy. CNC concentrations within the epoxy matrix were studied from CNC 0 wt% to CNC 0.9 wt%, in which the greatest increase in mechanical properties were observed at CNC 0.9 wt%. For the CNC 0.9 wt% composite, the tensile modulus increased by 25%, the tensile strength increased by 30%, the flexural modulus increased by 44% and the flexural strength increased by 33% as compared to the neat epoxy composites. The density measured for each of the CNC concentrations remained fairly constant for the

composites, indicating that the weight does not increase with the addition of CNC. These results highlight yet another scalable method in which CNC can enhance the mechanical properties of short-GF/epoxy SMC composites with no weight penalty for high volume composite production.

5.3 Future Work

While the results from these studies validate the usage of CNC to enhance polymer matrix composites, more work is necessary to determine the optimal incorporation method of CNC for manufacturing SMC. While WD-40 used in this study allowed for easy removal of the polyethylene sheeting, this solvent does not fully represent the improvements CNC has on the resulting composites. Other possible release agents should be tested and verified.

Although it has been shown that coating GF with CNC improves the macro-mechanical properties of the GF, the CNC bath must be used in conjunction with the SMC machine to verify that it can be a scalable process. In addition, the resulting composites must be characterized to ensure that the increase in mechanical properties is consistent with what was shown in the lab-scale study presented in this thesis. Further design work is necessary to ensure that the CNC bath is functional for usage, including utilizing high-temperature plastic rollers to reduce thread friction, an air-knife to facilitate spreading and drying within the bath, and ceramic eyes to guide the fibers into the SMC manufacturing line.

While the two methods have been verified individually as methods in which to incorporate CNC to enhance the macro mechanical properties of SMC, it is yet to be studied how these individual effects combined may affect the resulting composites.

Should each of the individual enhancements be compounded by combining the two methods, a hybridization of the two methods may prove to be a superior method for fully enhancing composites, and could lead to even more mechanical benefits greater than the ones stated in the previous sections.

The practicality of this project is based on light weighting composites without compromising their mechanical properties. It has been shown and validated through research that CNC can improve the mechanical properties of the resulting composites. However, now it is desired to know how much GF can be taken out of the composite while maintaining the mechanical properties of the composite given the addition of the CNC. More work must be done to quantify the light-weighting capability given the incorporation of CNC, such that there is a direct benefit of fuel efficiency for using CNC within SMC for the automotive and water vehicle industries.

REFERENCES

[1] Department of Energy US. Quadrennial Technology Review. 2011:39.

[2] Dorigato A, Morandi S, Pegoretti A. Effect of nanoclay addition on the fiber/matrix adhesion in epoxy/glass composites. Journal of Composite Materials. 2012;46(12):1439-1451.

[3] Pedrazzoli D, Pegoretti A, Kalaitzidou K. Synergistic effect of exfoliated graphite nanoplatelets and short glass fiber on the mechanical and interfacial properties of epoxy composites. Composites Science and Technology. 2014;98:15-21.

[4] Pedrazzoli D, Pegoretti A. Silica nanoparticles as coupling agents for polypropylene/glass composites. Composites Science and Technology. 2013;76:77-83.

[5] Gao SL, Mäder E, Plonka R. Nanocomposite coatings for healing surface defects of glass fibers and improving interfacial adhesion. Composites Science and Technology. 2008;68(14):2892-2901.

[6] Luo J-J, Daniel IM. Characterization and modeling of mechanical behavior of polymer/clay nanocomposites. Composites Science and Technology. 2003;63(11):1607-1616.

[7] Mallick, P. K. "Ch 8. Polymer Nanocomposites." *Fiber-reinforced Composites: Materials, Manufacturing, and Design*. 3rd ed. New York: M. Dekker, 2007. 575-98. Print.

[8] M. Kato and A. Usuki, Polymer–clay nanocomposites, in Polymer–Clay Nanocomposites
(T.J. Pinnavai and G.W. Beall, eds.), John Wiley & Sons, Chichester, UK (2000).

[9] H.R. Dennis, D.L. Hunter, D. Chang, S. Kim, J.L. White, J.W. Cho, and D.R. Paul, Effect of melt processing conditions on the extent of exfoliation in organoclaybased nanocomposites, Polymer, 42:9513 (2001).

[10] S.J. Ahmadi, Y.D. Huang, and W. Li, Synthetic routes, properties and future applications
of polymer-layered silicate nanocomposites, J. Mater. Sci., 39:1919 (2004).

[11] G.G. Tibbetts, M.L. Lake, K.L. Strong, and B.P. Price, A review of the fabrication and properties of vapor-grown carbon nanofiber=polymer composites, Composites Sci. Tech. 67:1709 (2007).

[12] I.S. Chronakis, Novel nanocomposites and nanoceramics based on polymer nanofibers
using electrospinning technology, J. Mater. Process. Tech., 167:283 (2005).

[13] Y.-Y. Fan, H.-M. Cheng, Y.-L. Wei, G. Su, and Z.-H. Shen, Tailoring the diameters of vapor-grown carbon nanofibers, Carbon, 38:921 (2000).

[14] I.C. Finegan, G.G. Tibbetts, D.G. Glasgow, J.-M. Ting, and M.L. Lake, Surface treatments for improving the mechanical properties of carbon nanofiber=thermoplastic composites, J. Mater. Sci., 38:3485 (2003).

[15] R.D. Patton, C.U. Pittman, Jr., L. Wang, and J.R. Hill, Vapor grown carbon fiber composites with epoxy and poly(phenylene sulfide) matrices, Composites: Part A, 30:1081 (1999)

[16] J. Han, Structure and properties of carbon nanotubes, Carbon Nanotubes: Science and Applications (M. Meyappan, ed.), CRC Press, Boca Raton, USA (2005).

[17] H.G. Chae, J. Liu, and S. Kumar, Carbon nanotube-enabled materials, Carbon Nanotubes: Properties and Applications (M.J. O'Connell, ed.), CRC Press, Boca Raton, USA, pp. 19–49 (2006).

[18] J.E. Fischer, Carbon nanotubes: structure and properties, Nanomaterials Handbook (Y. Gogotsi, ed.), CRC Press, Boca Raton, USA, pp. 69–103 (2006).

[19] J.N. Coleman, U. Khan, W.J. Blau, and Y.K. Gun'ko, Small but strong: a review of the mechanical properties of carbon nanotube–polymer composites, Carbon, 44:1624 (2006).

[20] X.-L. Xie, Y.-W. Mai, and X.-P. Zhou, Dispersion and alignment of carbon nanotubes in polymer matrix: a review, Mater. Sci. Eng., R49:89 (2005).

[21] B. Safadi, R. Andrews, and E.A. Grulke, Multiwalled carbon nanotube polymer composites: synthesis and characterization of thin films, J. Appl. Polym. Sci., 84:2660 (2002).

[22] W.D. Zhang, L. Shen, I.Y. Phang, and T. Liu, Carbon nanotubes reinforced nylon-6 composite prepared by simple melt compounding, Macromolecules, 37:256 (2004).

[23] Moon RJ, Martini A, Nairn J, Simonsen J, Youngblood J. Cellulose nanomaterials review: structure, properties and nanocomposites. Chemical Society Reviews. 2011;40(7):3941-3994.

[24] Lu J, Askeland P, Drzal LT. Surface modification of microfibrillated cellulose for epoxy composite applications. Polymer. 2008;49(5):1285-1296.

[25] R. Rusli, K. Shanmuganathan, S. J. Rowan, C. Weder and S. J. Eichhorn, Biomacromolecules, 2010, 11, 762–768.

[26] Pandey, Jitendra K., Antonio N. Nakagaito, and Hitoshi Takagi. "Fabrication and Applications of Cellulose Nanoparticle-based Polymer Composites." *Polym Eng Sci Polymer Engineering & Science* 53.1 (2012): 1-8.

[27] Al-Turaif, Hamad A. "Relationship between Tensile Properties and Film Formation Kinetics of Epoxy Resin Reinforced with Nanofibrillated Cellulose." *Progress in Organic Coatings* 76.2-3 (2013): 477-81.

[28] Low, I.m., M. Mcgrath, D. Lawrence, P. Schmidt, J. Lane, B.a. Latella, and K.s. Sim. "Mechanical and Fracture Properties of Cellulose-fibre-reinforced Epoxy Laminates." *Composites Part A: Applied Science and Manufacturing* 38.3 (2007): 963-74.

[29] Tang L, Weder C. Cellulose Whisker/Epoxy Resin Nanocomposites. ACS Applied Materials & Interfaces. 2010;2(4):1073-1080.

[30] P.K. Mallick, Sheet Molding Compounds, Composite Materials Technology (P.K. Mallick and S. Newman, eds.), Hanser Publishers, Munich (1990).

[31] Xu S, Girouard N, Schueneman G, Shofner ML, Meredith JC. Mechanical and thermal properties of waterborne epoxy composites containing cellulose nanocrystals. Polymer. 2013;54(24):6589-6598.

[32] Ruiz MM, Cavaillé JY, Dufresne A, Graillat C, Gérard J-F. New waterborne epoxy coatings based on cellulose nanofillers. Macromolecular Symposia. 2001;169(1):211-222.

[33] Peng SX, Moon RJ, Youngblood JP. Design and characterization of cellulose nanocrystal-enhanced epoxy hardeners. Green Materials. 2014; 2(4):193-205.

[34] Ansari F, Galland S, Johansson M, Plummer CJG, Berglund LA. Cellulose nanofiber network for moisture stable, strong and ductile biocomposites and increased epoxy curing rate. Composites Part A: Applied Science and Manufacturing. 2014;63:35-44.

[35] Barari B, Ellingham TK, Qamhia II, Pillai KM, El-Hajjar R, Turng L-S, et al. Mechanical characterization of Scalable Cellulose Nano-Fiber based Composites made using Liquid Composite Molding Process. Composites Part B: Engineering.In press.

[36] Miao C, Hamad WY. Cellulose reinforced polymer composites and nanocomposites: a critical review. Cellulose. 2013;20(5):2221-2262.

[37] Gabr MH, Elrahman MA, Okubo K, Fujii T. A study on mechanical properties of bacterial cellulose/epoxy reinforced by plain woven carbon fiber modified with liquid rubber. Composites Part A: Applied Science and Manufacturing. 2010;41(9):1263-1271.

[38] Chen Y, Zhou X, Yin X, Lin Q, Zhu M. A Novel Route to Modify the Interface of Glass Fiber-Reinforced Epoxy Resin Composite via Bacterial Cellulose. International Journal of Polymeric Materials and Polymeric Biomaterials. 2013;63(4):221-227.

[39] Postek MT, Moon RJ, Rudie AW, Bilodeau MA. Production and Applications of Cellulose.

[40] Girouard N, Schueneman GT, Shofner ML, Meredith JC. Exploiting colloidal interfaces to increase dispersion, performance, and pot-life in cellulose nanocrystal/waterborne epoxy composites. Polymer. 2015;68:111-121.

[41] Hunston D, McDonough W, Holmes G, Parnas R, Drzal L, Rich M. Test Protocol for Single-Fiber Fragmentation Test International Round Robin.

[42] Kelley A, Tyson W. Tensile Properties of Fiber-Reinforced Metals. Journal of Mechanical and Physical Solids. 1965;13:329-350.

[43] Mullin JV, Mazzio VF. The effects of matrix and interface modification on local fractures of carbon fibers in epoxy. Journal of the Mechanics and Physics of Solids. 1972;20(6):391-394.

[44] Zhou XF, Nairn JA, Wagner HD. Fiber–matrix adhesion from the single-fiber composite test: nucleation of interfacial debonding. Composites Part A: Applied Science and Manufacturing. 1999;30(12):1387-1400.

[45] Hashin Z. Thermoelastic properties of fiber composites with imperfect interface. Mechanics of Materials. 1990;8(4):333-348.

[46] Nairn JA. Generalized shear-lag analysis including imperfect interfaces. Advanced Composites Letters. 2004;13(6):263-274.

[47] Gao S-L, Mäder E. Characterisation of interphase nanoscale property variations in glass fibre reinforced polypropylene and epoxy resin composites. Composites Part A: Applied Science and Manufacturing. 2002;33(4):559-576.

[48] Madhukar MS, Drzal LT. Fiber-matrix adhesion and its effect on composite mechanical properties: II. Longitudinal (0) and transverse (90) tensile and flexure behavior of graphite/epoxy composites. Journal of Composite Materials. 1991;25(8):958-991.

[49] Low IM, McGrath M, Lawrence D, Schmidt P, Lane J, Latella BA, et al. Mechanical and fracture properties of cellulose-fibre-reinforced epoxy laminates. Composites Part A: Applied Science and Manufacturing. 2007;38(3):963-974.

[50] Asadi A, Miller M, Moon RJ, Kalaitzidou K. Improving the interfacial and mechanical properties of short glass fiber/epoxy composites by coating the glass fibers with cellulose nanocrystals Express Polymer Letters. 2015;Under review.

[51] Mallik PK. Fiber-reinforced composites: materials, manufacturing and design. 3 ed. Florida, USA: CRC Press, Taylor & Francis Group; 2007.